

The Scheelite Skarn Deposit of Salau (Ariege, French Pyrenees)

MICHEL FONTEILLES,

Centre National de la Recherche Scientifique, Pétrologie (Eruptive et Métamorphique), Magmatologie et Métallogénie, Université Pierre et Marie Curie, 4 place Jussieu, 75005 Paris, France

PIERRE SOLER,

Institut Français de Recherche Scientifique pour le Développement en Coopération—ORSTOM, 213 rue Lafayette, 75010 Paris, France, and Laboratoire de Géochimie Comparée et Systematique (Université Pierre et Marie Curie, Paris)

MICHEL DEMANGE,

Centre National de la Recherche Scientifique, Pétrologie (Eruptive et Métamorphique), Magmatologie et Métallogénie, Université Pierre et Marie Curie, 4 place Jussieu, 75005 Paris, France, and Centre de Géologie Generale et Minière, Ecole des Mines de Paris, 60 Boulevard Saint Michel, 75006 Paris, France

COLETTE DERRÉ,

Centre National de la Recherche Scientifique, Pétrologie (Eruptive et Métamorphique), Magmatologie et Métallogénie, Université Pierre et Marie Curie, 4 place Jussieu, 75005 Paris, France, and Laboratoire de Géologie Appliquée, Université Pierre et Marie Curie, 4 place Jussieu, 75005 Paris, France

ANNE DOMINIQUE KRIER-SCHELLEN, JEAN VERKAEREN,

Laboratoire de Minéralogie et Géologie Appliquée, Université Catholique de Louvain, 3 place Louis Pasteur, 1348 Louvain-la-Neuve, Belgium

BERNARD GUY, AND ALAIN ZAHM

Centre National de la Recherche Scientifique, Pétrologie (Eruptive et Métamorphique), Magmatologie et Métallogénie, Université Pierre et Marie Curie, 4 place Jussieu, 75005 Paris, France, and Laboratoire de Géologie, Ecole des Mines de Saint Etienne, 158 cours Fauriel, 42000 Saint-Etienne, France

Abstract

Between 1971 and 1986 the scheelite deposit of Salau, located in the French Hercynian Pyrenees, produced 930,000 metric tons of ore with 1.50 percent WO_3 (13,950 metric tons of WO_3).

The skarn deposit is hosted in a Devonian carbonate and partly detrital series intruded by a late Carboniferous stock. In the Devonian series (the lithostratigraphy and geochemistry of which is described in some detail) a unit of so-called "Barregiennes" (i.e., rhythmic alternations of limestones and silts) appears to be very favorable for extensive development of skarns and overprinted ores.

The Hercynian orogeny involved polyphase deformation, regional metamorphism of greenschist facies, and late intrusions of granite-granodiorite. Deformation included two coaxial stages of tight isoclinal folding and one important later stage which partly controlled the intrusion of the granodiorite stock, followed by three stages of brittle deformation. Ore deposition is related to faulting stages 0 and 1 and orebodies are cut into slices by stage 2 reverse faults.

The Salau intrusion includes various rock types belonging to two slightly different calc-alkaline trends. One of these trends, characterized by its low K contents, is unusual in the Pyrenees. The local shapes of the intrusion, apophyses and embayments, are important controls of the orebodies.

After isochemical contact metamorphism, the skarns and ores developed in two main stages related to the infiltration of two quite different types of fluids. During the first stage (540°–450°C), anhydrous skarn formation was followed by an intergranular development of pyrrhotite-scheelite-quartz-calcite in equilibrium with the earlier hedenbergite. The resulting tungsten grade is uneconomic. The associated fluids, probably of magmatic origin, had a high salinity. In the second stage (450°–350°C), no new skarn formed; transformations of the silicate rocks are observed. A first substage of epidotization was followed by the development of intermediate grossularite-almandine-spessartite garnet and finally by the main ore stage

17 JULI 1995

ORSTOM Fonds Documentaire

N° 541863 ed. 4

Cote : 5

with scheelite, pyrrhotite, arsenopyrite, and other sulfides with some gold. Two types of fluid inclusions are found in this stage; one is similar in composition to the first stage, the other is characterized by low salinity and high CO_2 and CH_4 contents.

Introduction

THE Salau mine is located in the central part of the French Pyrenees near the spring of the Salat River, 130 km south of Toulouse, 30 km south of Saint Giron, and 4 km north of the Spanish border (Fig. 1). The deposit was discovered in 1961 during a regional strategic prospection campaign held by the French Bureau de Recherches Géologiques et Minières (BRGM). Mineralized outcrops are known between altitudes of 1,230 and 1,850 m.

The tungsten ore was exploited by the Société Minière d'Anglade from April 1971 to November 1986. The Salau mine has been the main French tungsten producer during this period with a total of nearly 930,000 metric tons of ore with 1.50 percent WO_3 (i.e., $\approx 13,950$ metric tons WO_3). Due to the drop in the price of tungsten, mining operation ceased in November 1986. At the time of shutdown the proved and probable workable reserves were more than 160,000 metric tons of ore with nearly 1.75 percent WO_3 (i.e., $\approx 2,800$ metric tons WO_3), and extensions of the orebodies at depth were demonstrated.

The orebodies are located at or near the contact between a Hercynian granodioritic intrusive stock (the La Fourque stock), and folded and metamorphosed carbonate sedimentary rocks of Silurian and Devonian age. Scheelite occurs mainly in skarns modified by late hydrothermal processes and partly in mylonites inside the granodiorite. The geometry of the orebodies is complex and appears controlled mainly by irregularities in the intrusive contact and faults.

The present paper is a synthesis of numerous studies undertaken on the Salau deposit for the last 20 years since the early work by Fonteilles and Machairas (1968). The most important contributions have been by Soler (1977), Derré (1978, 1982), Autran et al. (1980), Raimbault (1981), Kaelin (1982), Zahm (1987a), Fonteilles et al. (1988), Guy et al. (1988), and Krier-Schellen (1988). The present paper is a synthesis of these results including regional geologic setting, lithostratigraphy, and geochemistry of the sedimentary country rocks, regional metamorphism, folding and brittle deformation, geometry of the intrusive rocks and the orebodies, petrography and geochemistry of the intrusive rocks, petrography and mineralogy of contact metamorphic, metasomatic, and hydrothermal rocks, P-T-X conditions at the different stages of the formation of the deposit, fluid inclusions, and stable isotopes.

Regional Geologic Setting

The Pyrenees are an alpine chain (Upper Cretaceous-Eocene) superimposed on Paleozoic terrains with a Precambrian basement, deformed during Hercynian orogeny. Alpine deformation of the Paleozoic rocks is mostly limited to thrusting and faulting.

Pyrenean pre-Hercynian sedimentary series

The Pyrenean pre-Hercynian sedimentary series are reported as three major Paleozoic sedimentary cycles, in some cases concordant but generally separated by disconformities on a regional scale and even locally by angular unconformities. The Precambrian basement consists of paragneisses (1,569 Ma by the

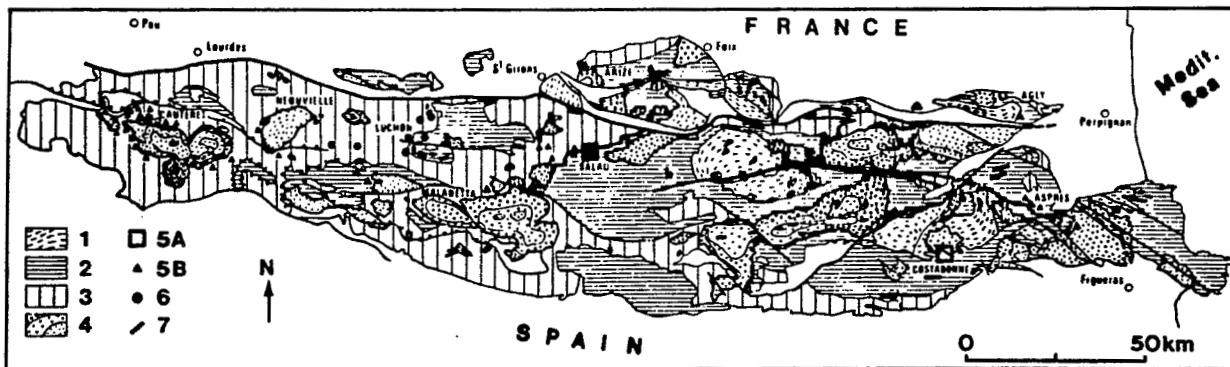


FIG. 1. Geologic map of the Hercynian Pyrenees. Localization of the principal tungsten ore deposits and occurrences (modified from Autran et al., 1980). 1 = upper Proterozoic basement, 2 = Cambrian and Ordovician, 3 = Silurian, Devonian, and Carboniferous, 4 = Upper Westphalian Granitoids (with the limits of the petrographical types for the composite massives: heavy dots = basic, light dots = acid), 5 = skarn scheelite deposits (A) and occurrences (B), 6 = other scheelite occurrences (calcite-quartz-scheelite veinlets), 7 = quartz-arsenopyrite-wolframite-gold veins.

Nd-Sm method; Ben Othman et al., 1984) intruded by late Proterozoic granitoids (now orthogneisses) dated at 630 Ma (Rb-Sr method; Vitrac-Michard and Allègre, 1975). The Cambrian-Lower Ordovician sedimentary cycle began with a platform volcano-sedimentary, detrital, and carbonate sequence with some interbedded black shales ("Canaveilles group"), followed by a very thick detrital sequence ("Jujols group") (Guitard, 1970; Laumonier and Guitard, 1986). The Upper Ordovician-Silurian cycle began again with platform sedimentation: mostly detrital (in some cases coarse grained), with carbonate intercalations and, very locally, intermediate to rhyolitic volcanism of calc-alkaline affinity, then, a rather uniform euxinic basin developed during the Silurian (Cavet, 1957; Fonteilles, 1976). The Devonian-Carboniferous cycle began equally with mostly platform carbonate (and locally detrital) sedimentation (Lower Devonian), then evolved to a slope sedimentation during the Upper Devonian and to pelagic sedimentation with radiolarites during the lowermost Carboniferous; flysch-type sedimentation predominated during lower Carboniferous times. The Hercynian tectonics has brought close together two very different isopical domains. The allochthonous Devonian is made of very thick platform carbonate series, whereas the autochthonous Devonian series is thin and mainly composed of calc-schists of distal character.

Notwithstanding the existence of black shales in each of these Paleozoic sedimentary cycles and abnormal concentrations of Zn, Pb, Ba, and Cu in the Upper Ordovician and Lower Devonian formations, no concentration of tungsten higher than 2 ppm has been detected in the Pyrenean Paleozoic series (Derré, 1982). The tungsten showings and deposits, which are mostly of skarn type (Fig. 1), are restricted to carbonate formations, Cambrian as well as Lower Ordovician and Devonian in age.

Hercynian orogeny

The Hercynian orogeny occurred in the Pyrenees between Namurian and D-Westphalian. The earliest phases of folding produced mostly similar folds contemporaneous with metamorphism and foliation; some very deep-seated nappes, pennic in style, were formed in the eastern part of the chain (Guitard, 1964; Autran and Guitard, 1969). The later phases resulted in folds with steeply dipping axial planes. The interference of two important phases striking N 110° E and N 70°-80° E, respectively, formed a basin and dome structure. Deep-seated terranes, in particular the Precambrian basement, appear in the core of flattened domes, along the flanks of which the rocks are isoclinally folded and dip vertically (Guitard, 1970; Boissonnas and Autran, 1974; Laumonier and Guitard, 1986). Precise dating of the Devonian sedimentary formations (Raymond, 1980; Cygan et al., 1981)

demonstrates the existence of large thrusts which involve Devonian platform formations and some lower Carboniferous rocks; those thrusts postdate the early folding but are refolded by the later phases.

Syntectonic metamorphism, which grades from epizonal to granulite facies, is typically of low-pressure type and is remarkably controlled by a basement effect of the Precambrian domes as defined by Fonteilles and Guitard (1974).

Besides numerous small bodies of peri-anatectic granites and pegmatites and some catazonal or mesozonal stocks, most of the Hercynian plutonism of the Pyrenees is represented by batholiths emplaced at a rather high level in the crust (Autran et al., 1970). The roof of these massifs reaches the chlorite zone of regional metamorphism (commonly Silurian and Devonian terranes). Rb-Sr dating gives ages in the range of 290 to 270 Ma (Vitrac-Michard and Allègre, 1975).

These composite batholiths are mostly made of granodiorites and adamellites but include some more mafic rocks (tonalites, diorites, gabbros, and cordlandites) and some more felsic rocks (muscovite- or tourmaline-bearing granites) (Autran et al., 1970). These plutons define a typical continuous calc-alkaline suite from the gabbros to the evolved granites. Several individual trends may be distinguished on the basis of more or less sodic or potassic character, and of Fe and Al contents vs. MgO or TiO₂. Tungsten occurrences of the Pyrenees are almost exclusively of skarn type spatially associated with these intrusions (Autran et al., 1980; Fig. 1). There is no occurrence either of tin or niobium-tantalum.

There is no obvious relation between the W deposits and the chemistry (within the granitoid family) of the intrusions. The main controls appear to be the shape (apical character, morphology of the contacts), scale, and level of emplacement of the intrusions (i.e., the thermal disequilibrium between the intrusion and the host rocks).

Sedimentary Host Rocks

Lithostratigraphy

The Salau scheelite deposit is located on the northern flank of the Pallaresa anticline (Fig. 2) which is made of lower Paleozoic terranes. The sedimentary rocks strike east-west and dip vertically. Disregarding the minor folds, the oldest terranes crop out in the south and the youngest in the north. From south to north, one may distinguish (Fig. 3) the following formations: (1) the pelito-psammitic Mont Rouch Formation, which is inferred to be of Lower to Middle Ordovician age (Zandvliet, 1960; Dommangot, 1977; Palau et al., 1989); (2) the Salau Formation, which has not been dated locally but its lateral equivalent in the Marimaña area provided conodonts with ages ranging from Upper Silurian to Lower Devonian; it

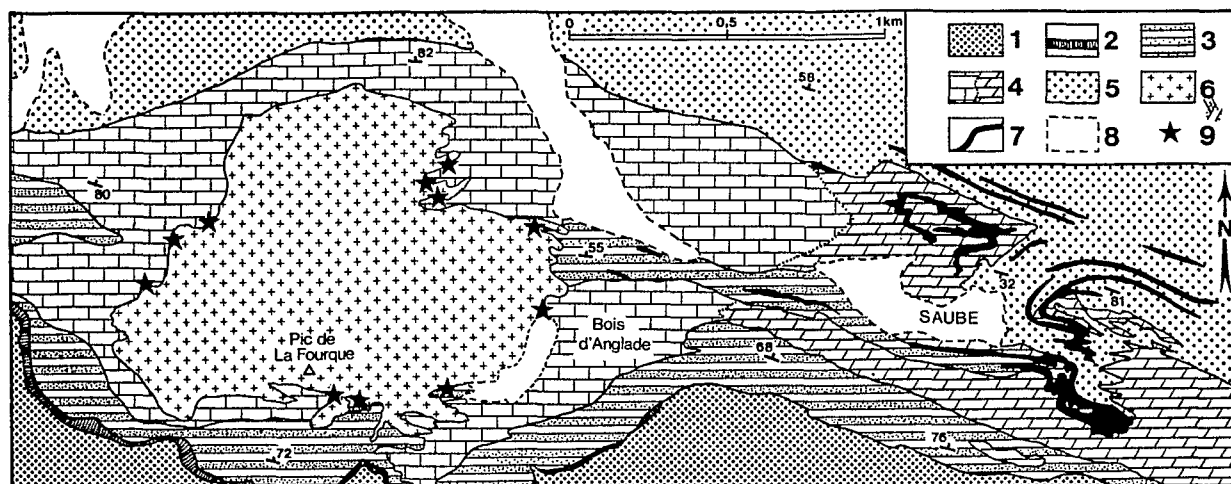


FIG. 2. Geologic map of the Salau area and localization of the scheelite bearing skarns around the La Fourque stock (from Derré, 1982 and modified from L. Nansot, Société Minière d'Anglade unpub. data). 1 = pelito-psammitic Mont Rouch Formation (Lower to Middle Ordovician); Salau Formation (Upper Silurian to Emsian); 2 = Black unit, 3 = Barrégiennes unit, 4 = carbonate Salau unit; 5 = Blue Shales Formation (Efelian); 6 = La Fourque granodioritic stock; 7 = microgranitic or microgranodioritic sills and dikes; 8 = Quaternary deposits; 9 = scheelite-bearing skarns. Numbers (80, 72, etc.) indicate dip of the stratification.

includes the clastic and carbonate basal Black unit; a rhythmic alternation of pelites and limestones, known locally as the "Barrégiennes" (Caralp, 1888) of Upper Silurian age (probably lower Ludlow, Losantos et al., 1985); and the carbonate unit of Salau, the upper part of which is laterally dated of Emsian age (Moret and Weyant, 1986); (3) the Blue Shales Formation of Efelian age (Moret and Weyant, 1986); and (4) the carbonate Carboire Formation of Lower to Middle Devonian age (Dommanget, 1977).

To the north the Salau and Blue Shales Formations are separated from the Carboire Formation of the same age which, however, belongs to a different isopical zone by a major thrust which was folded by the late tectonic phases.

Black carbonaceous shales are the classical Silurian facies in the Pyrenees. Because such shales are not known between the Salau Formation and the lower Mont Rouch Formation, various authors (Moret and Weyant, 1986; Bodin and Ledru, 1986) consider that there is a major thrust between these formations. This abnormal contact can be traced up to the thrust described by Palau et al. (1989) in the south of the Marimaña massif. However, detailed observation of the contacts does not produce clear evidence of such a major abnormal contact in the Salau area. Moreover, the identical chemistry of both series (see below) and the fact that, in the mine, the Mont Rouch Formation and the Salau Formation are involved in early isoclinal folds which are supposed to predate the inferred thrust, support the hypothesis that this contact is a normal one. The variety of facies in the Black unit at

the base of the Salau Formation, and the fact that this unit lies on different units of the Mont Rouch Formation may also be interpreted as a disconformity.

Mont Rouch Formation: This formation represents the top of the thick lower Paleozoic series which crops out in the core of the Pallaresa anticline. At the Cruzous pass, some 2 km east of the deposit, three units may be distinguished: a lower unit of gray laminated pelites; a unit of rather pure quartzites and green pelites with some intercalations of sandy dolomites and conglomerates (400–500 m); and a unit of banded sandy shales (30 m at the Cruzous Pass, 120 m south of the deposit) with some more calcareous beds and some shales with sulfides (pyrite, pyrrhotite, sphalerite, chalcopryrite). Sedimentological, petrographical, and geochemical features assign this formation to a platform environment.

Salau Formation: The basal Black unit is a carbonate and detrital formation, with important lateral variations, but always rich in organic matter, and in some cases, in phosphate (Derré and Krylatov, 1976; Kaelin, 1982). The facies are roughly organized both vertically—from clastic at the base to biochemical at the top (carbonaceous carbonates)—and horizontally—from a proximal shallow area eastward (coarse detritals and dolomites) to a more distal area westward (black shales and limestones with sulfides). These black sedimentary rocks were deposited in a euxinic environment with important biochemical activity.

The Barrégiennes unit is a very regular unit consisting of rhythmic alternation of detrital and carbonate layers. The thickness of the individual detritic

regime. These shales contain quartz, muscovite, chlorite, graphite, and sulfides. Chloritoid is common and locally abundant. Margarite and/or epidote appear in the lower part of the formation.

A calc-schist unit of about 10 m in thickness occurs in the lower part of the formation; crinoids are common and locally form true encrinites at the top of this unit. This carbonate unit disappears westward in the vicinity of the mine and grades eastward to dolomites.

Carboire Formation: This formation overlies conformably, with a tectonic contact, the Blue Shales Formation. Its base consists of gray to black limestones with some calcareous sandy shales (50 m), overlain by black graphitic shales followed by limestones and shales alternating in centimetric to decimetric beds. These limestones are mineralized with Zn and Pb at Carboire, Saubé, and Hoque Rabé to the east of Salau and at Bonabé in Spain (Charreau, 1974; Dommangeat, 1977).

Geochemistry

The sedimentary rocks of the Salau area have undergone regional epizonal metamorphism as discussed below. The sedimentary textures and mineralogy are commonly blurred and the aim of the geochemical analysis is to reconstruct the primary sedimentary assemblages. The 118 analysis of sedimentary rocks sampled far from the deposit are classified into two groups: rocks with free carbonates (i.e., primary sedimentary carbonates), even in small amounts (diagram Na_2O vs. CaO ; Fig. 4), and rocks free of carbonate: shales and sandstones. Among these, different types may be distinguished. The diagram $\text{Na}_2\text{O} + 31/47 \text{K}_2\text{O}$ vs. Al_2O_3 (Fig. 5) illustrates the repartitioning of alumina between feldspars and phyllites; the dia-

gram $\text{K}-(\text{Fe} + \text{Mg})-(\text{Al}-\text{Na}-2\text{Ca})$ (i.e., nonfeldspathic alumina; Fig. 6) may be used for discussion of the clay minerals. On the MgO vs. Fe_2O_3 diagram (Fig. 7), a special group can be recognized by its high Mg content.

Detrital rocks free of carbonate or with very low carbonate content: These rocks (from the Mont Rouch, Salau, and Blue Shales Formations) form a bimodal population: sandstones and shales. The high silica content of the sandstones (>70%), their low alumina content (<12%), and their high $\text{Al}/(\text{Na} + \text{K})$ ratio exclude the presence of arkoses and graywackes; the sandstones belong to the lithic arenites class (Pettijohn et al., 1972). The shales are rich to very rich in alumina (18–32%) and their $\text{Al}/(\text{Na} + \text{K})$ ratios are high. This Al-rich shale-lithic arenites association is typical of platform sedimentation (Pettijohn et al., 1972). Further analysis shows that the detrital formations of the Salau area belong to distinct sedimentary ensembles. The lower group includes the Mont Rouch Formation and the noncarbonate detrital rocks of the Salau Formation, whereas the upper one corresponds to the Blue Shales Formation (Figs. 5 to 7 and Table 1).

Carbonate rocks: The carbonate rocks correspond to a mixture between two independent components: carbonates and silico-aluminous detritus. The presence of free carbonates may be inferred for samples in which the CaO content is higher than 1.3 to 1.4 percent (Fig. 4). The range of CaO content is 1.3 to 56 percent. As far as the detrital fraction is concerned, one can recognize a bimodal distribution between shales and sandstones observed in the purely detrital rocks and the existence of two successive series as described in the previous section. The presence of

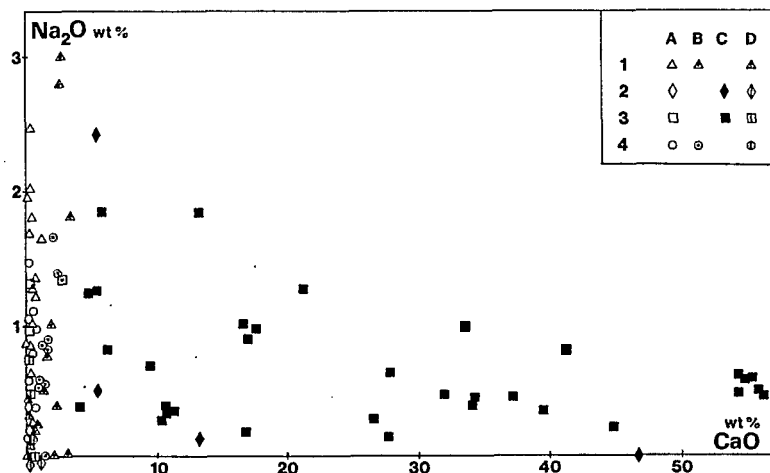


FIG. 4. Na_2O vs. CaO diagram for sedimentary rocks of the Salau area. Symbols: A = noncarbonate sandstones and shales, B = sandstones and shales with very low carbonate content, C = carbonate rocks, D = Mg-rich noncarbonate rocks; 1 = Mont Rouch Formation, 2 = Black unit, 3 = Barréennes and Salau units, 4 = Blue Shales Formation.

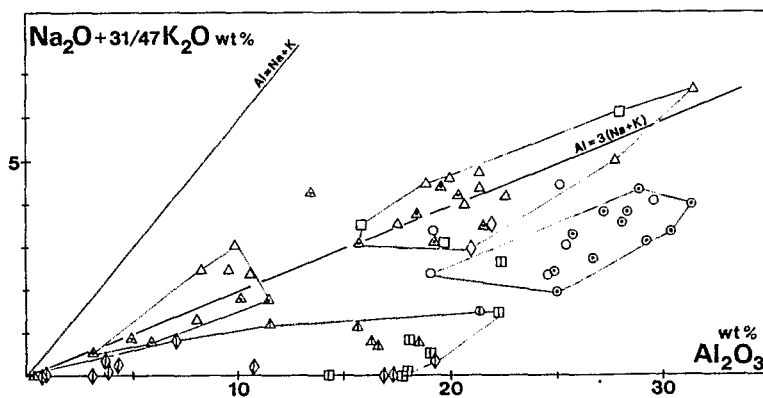


FIG. 5. $\text{Na}_2\text{O} + 31/47 \text{K}_2\text{O}$ vs. Al_2O_3 diagram for non-carbonate sedimentary rocks of the Salau area. Symbols as in Figure 4.

some dolomite in those carbonate rocks results in a slightly lower Fe/Mg ratio than in the corresponding detrital rocks (Fig. 7).

Paleogeographic conclusions

The Salau Formation appears as a positive megasequence with the following succession (with some re-

currences): detrital facies, first coarse then fine-grained; rhythmic alternation of clastics and carbonates, with a progressive decrease in the proportion of clastic material; and nearly pure carbonates. Geochemical data would indicate that the Mont Rouch Formation participated in this large cycle. The change from the Mont Rouch Formation to the Salau Formation corresponds with a rapid increase of chemical-biochemical sedimentation which dilutes gradually

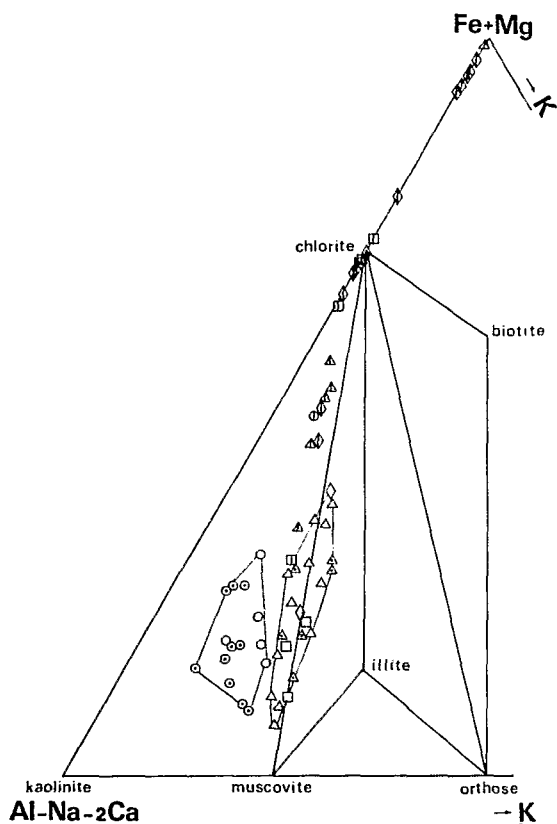


FIG. 6. Triangular Fe + Mg-Al-Na-2Ca-K diagram for the noncarbonate sedimentary rocks of the Salau area. Symbols as in Figure 4.

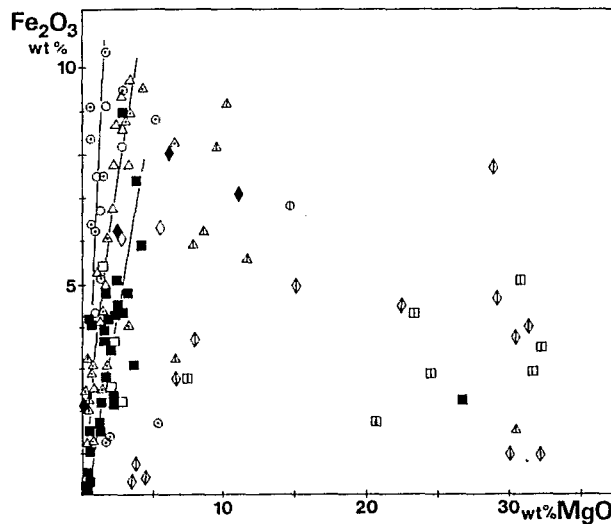


FIG. 7. Fe_2O_3 vs. MgO diagram for the sedimentary rocks of the Salau area. Symbols as in Figure 4. Noncarbonate rocks with high Mg contents are clearly distinguished in this diagram. They appear in all the series but are volumetrically subordinate. Three groups may be distinguished (see Fig. 6): (1) a group chemically intermediate between common detrital rocks and chloritites, (2) chloritites, and (3) talc + chlorite rocks. Textures, in particular the lack of foliation in these rocks, show that they are probably of a metasomatic-hydrothermal origin. They appear to be similar to other metasomatic talc or chlorite deposits and occurrences known in the Pyrenees.

TABLE 1. Main Characteristics of Noncarbonate Rocks of the Mont Rouch, Salau, and Blue Shales Formations

	Mont Rouch and Salau Formations	Blue Shales Formation
Petrography	Lithic arenites + shales	High alumina shales
Al/Na + K	≈3	5 (up to 8.75)
Reconstructed phyllite association	Muscovite + chlorite	High kaolinite content
Fe/Fe + Mg		
Sandstones	0.70	
Shales	0.60–0.65	0.70–0.88
Ca/Ca + Na (rocks without free sedimentary carbonates)	0.15	0.20–0.30

the detrital supply. The volume of the latter decreases with time, but its nature does not vary all along the cycle. These facts deny any importance to the unconformity between both series and make very improbable the hypothesis of an important thrust between them. The Blue Shales Formation belongs to a different sedimentary cycle where the source areas appear to have been much more mature.

Local Geologic Evolution and Geometry of the Deposit

Folding phases

Considering their importance as a control on ore distribution, fold structures have been studied by Derré (1973, 1978), Charuau (1974), Soler (1977), Soler and Fontelles (1980a), and more specifically by Kaelin (1982). The successive tectonic phases recognized in the present paper may be easily correlated with the regional tectonic events (Deramond, 1970; Boissonnas and Autran, 1974).

Fold structures are difficult to decipher in the mine due to the effects of the granodiorite intrusion, mineralization, and brittle deformation. Therefore the structural study was carried out on the eastern slope of the Cougnets valley facing the mine, away from the granite; the structures unraveled there were traced westward to the mine.

Seven tectonic phases have been recognized but only three of these, P₁ to P₃, appear important:

P₀. Prefoliation phase, only demonstrated by the dispersion of the axis of the later phases in their axial plane. The reconstructed folds are open folds with a subhorizontal axis, trending N 45° E. This phase explains the axial culminations and plunges of the later structures.

P₁. This synfoliation phase of regional extent gives isoclinal recumbent folds, of plurihctometric to kilo-

metric amplitude with a northward vergence. The fold axes, almost horizontal, trend N 110°–120° E in the area east of the mine where they are undisturbed by the later phases (Fig. 8A and B). The associated foliation is more or less penetrative and largely transposes the bedding (graphitic banding of the marbles, calc-silicate hornfelses) with some metamorphic differentiation (Zahm, 1987a).

P₂. This phase, practically coaxial with P₁, formed centimetric to plurihctometric, horizontal, normal tight folds with rounded hinges and vertical limbs. The axial plane is deformed by subsequent deformational phases, trends 120° E, and dips from 70° NE to 60° SW. A strain slip or fracture foliation developed in narrow belts in the major hinge zones. This phase is responsible for the regional vertical dip of the series. It interferes with P₁, forming remarkable "en lacets" interference patterns of cartographic scale (Figs. 2 and 8A).

P₃. This phase formed nearly horizontal normal folds with subvertical axial planes trending N 150° E and a rough fracture foliation. The folds appear restricted to narrow belts. In the mine area, this phase was responsible for a major change in the trend of former structures from N 120° E to N 40° E (Fig. 8A). The La Fourque stock is located in such a belt of P₃ folds.

Regional metamorphism

The Paleozoic country rock of the Salau deposit has undergone a regional low-grade syntectonic metamorphism of greenschist facies. The common pelitic rocks show the association quartz-muscovite-chlorite ± albite. Epidote is present in the more calcareous beds. Fe- and Al-rich pelites of the Blue Shales Formation commonly contain chloritoid and the more calcareous beds of this series contain margarite. A regional biotite isograd is not reached in the Salau area.

Folds in the deposit

The deposit is located in the southern border of the La Fourque granodioritic stock, at the periphery of a P₂ anticline trending N 70°–90° E which culminates in the center of the mine and plunges eastward and westward. This anticline refolded the large P₁ recumbent folds (Figs. 9 and 10). Between the 1350 and 1500 levels, the core of this P₂ anticline consists of shales of the Mont Rouch Series involved in a P₁ recumbent fold. In the eastern part, those shales are invaded by the granodiorite. This major structure is complicated by minor parasitic folds which appear to control the detailed geometry of the intrusive contact. This P₁ × P₂ structure is deformed by transverse folds trending N 140°–150° E, related to the P₃ phase (Fig. 9). Those P₃ structures partly control the geometry of the apophyses of the granodiorite.

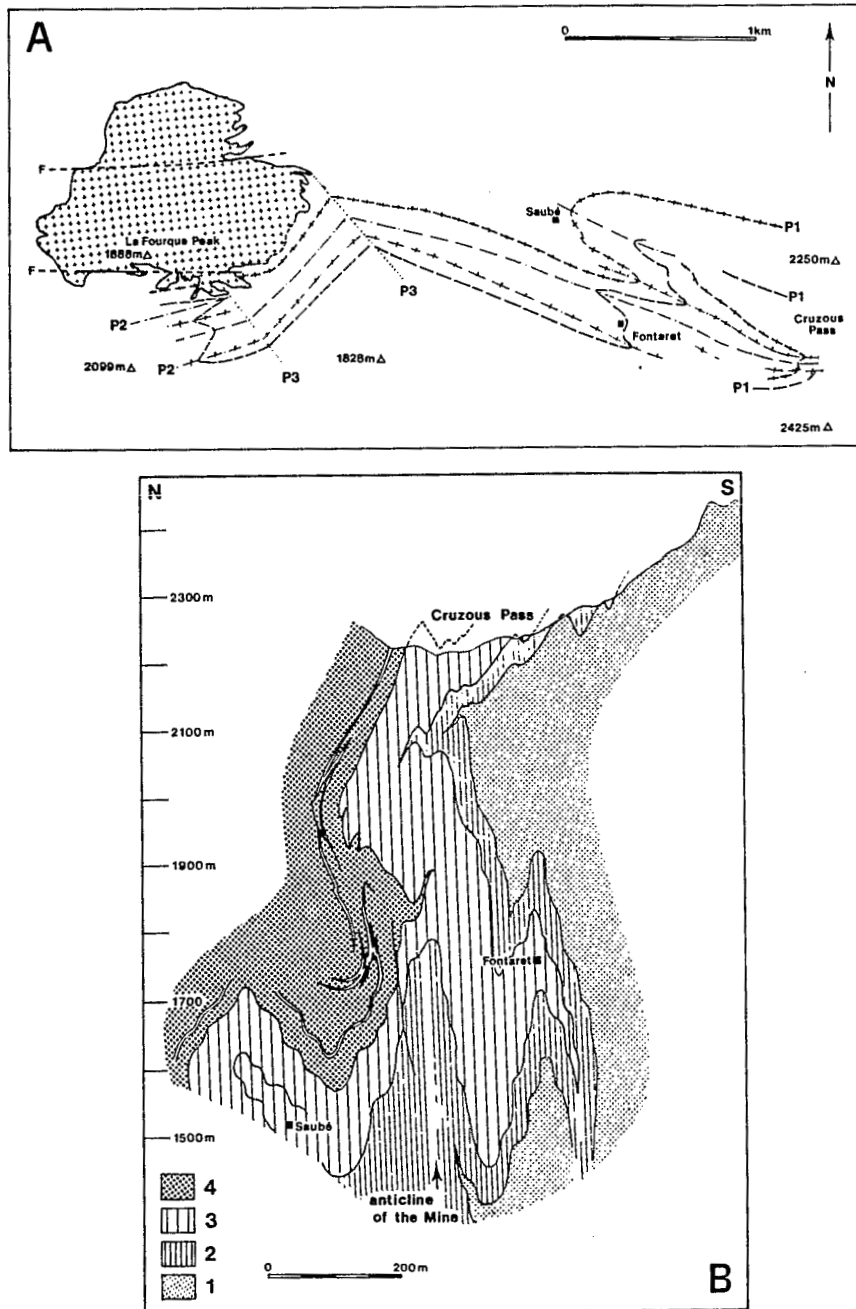


FIG. 8. Regional structures in the eastern part of the Salau area. A. Structural map. B. Synthetic normal cross section of the homoaxial folded structure integrating parallel cross sections at different levels in the eastern slope of the Cougnets valley facing the mine. 1 = Mont Rouch Formation, 2 = Barrégiennes and Black units, 3 = Salau unit, 4 = Blue Shales Formation. P₁, P₂, P₃ = axial planes of folding phases, F = faults.

Dimension and shape of intrusions

Intrusive rocks in the Salau area include the La Fourque stock and a series of sills and dikes.

The La Fourque stock has an equidimensional outcrop (1 km N-S; 1.2 km E-W; Fig. 2). Field obser-

vations are restricted because of the very steep topography and difficulty of access in the central and southern part of the stock, and debris and vegetation in its northern part. The best studied area is its south-eastern part in the mine area.

The shape of the southern contact is very compli-

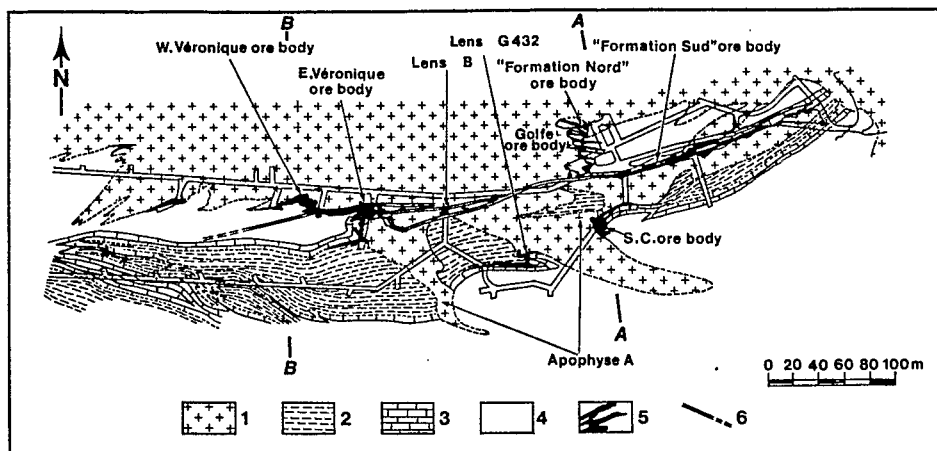


FIG. 9. Map of the 1430 level (modified from Derré, 1982). 1 = intrusive rocks, 2 = metamorphized Mont Rouch shales, 3 = marbles and limestones, 4 = calc-silicate hornfels (metamorphized Barrégiennes), 5 = skarns and orebodies, 6 = principal faults; AA = cross section of the Bois d'Anglade, BB = cross section of Véronique.

cated in detail (Figs. 9 to 13), with many apophyses and embayments which play an important role with respect to skarn location (zones V and VI and Bois d'Anglade embayment; Fig. 14). In the mine the contact is generally very steep with a few apophyses well known by mining: apophysis A, known below the 1475 level, is vertical, trends south, and broadens downward (Figs. 9 and 14); apophysis B, known between the 1485 and 1520 levels, is subhorizontal and overlies the Véronique skarns and orebodies (Fig. 14). Considered as a whole, below the 1485 level, the contact in the mine dips north, but this is largely the result of reverse faulting as discussed in the next section (Fig. 10). In the embayment structures, the shape of the contact between granodiorite and carbonates is in many places narrowly controlled by folds and was inherited from a previous stratigraphic contact since the intrusion mostly replaces silico-aluminous rocks of the Mont Rouch Formation.

The shape of the northern contact is not so well known, but it is probably as complex as the southern one, with embayments, such as the Christine showing (see below). Drilling in the western area indicates that the contact plunges southward.

Many sills are known mostly east of the mine, in a narrow east-west-trending zone between the La Fourque stock and the Bassies massif (Figs. 1 and 2). The shape of the contact metamorphic zone (see below) is very elongated along the same east-west direction. These sills, described by Zandvliet (1960), have a thickness of 1 to 10 m and their length may reach a few hundred meters. They are folded (Fig. 2) and are probably earlier than the La Fourque intrusion.

Minor dikes are known in the mine area and are

probably more directly linked to the La Fourque intrusion.

Emplacement of the La Fourque stock clearly postdates the P_2 folds. As pointed out above, the P_3 structures appear to partly control the location of the apophyses and even the location of the La Fourque stock. Since the granite is affected by all the known phases of brittle deformation, the emplacement of this stock may be syn- or late P_3 .

Brittle deformation within the deposit

A series of nearly east-west fault planes has been identified in the mine (Soler, 1977; Kaelin, 1982; Lecouffe, 1987; Fonteilles et al., 1988), mainly along the northern border of the main $P_1 \times P_2$ anticline. The earliest ones among these structures play an important role with respect to the distribution of skarns and orebodies, whereas the latest cut and offset the orebodies. In detail, at least three families of such faults are known (F_0 , F_1 , F_2) with slightly different orientations:

1. F_0 faults correspond to early mylonites trending $N 90^\circ - 120^\circ E$ (Fig. 13). Kaelin (1982) describes P_3 -like folds affecting them. Those mylonites are subvertical and 3 to 5 m thick. They are only known in the Véronique orebodies.

2. F_1 structures trend $N 80^\circ - 90^\circ E$, dip $70^\circ - 80^\circ N$, and appear as faults only in the silicate rocks (granodiorite, Mont Rouch Formation). In the carbonate rocks they give way to plastic flow and disharmonic folds.

3. F_2 are reverse faults trending $N 80^\circ - 140^\circ E$ (mean trend 120°) and dipping $40^\circ - 80^\circ N$. They are filled with quartz, calcite, amphibole, and some

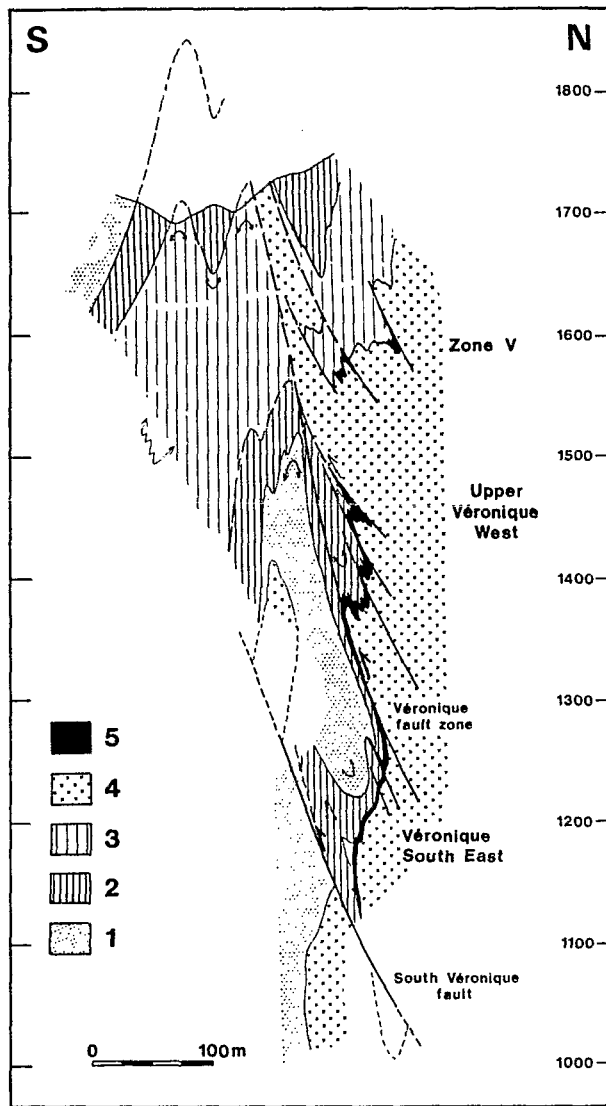


FIG. 10. Vertical north-south cross section of the Véronique orebodies (modified from L. Nansot, Société Minière d'Anglade unpub. documents). 1 = Mont Rouch Formation, 2 = Barréziennes and Black units, 3 = Salau Formation, 4 = intrusive rocks, 5 = ore. Location of the cross section is BB in Figure 9.

scheelite in large crystals without economic interest. They cut and offset the orebodies. The main F_2 fault zone, called the Véronique fault, cuts the deposit (Figs. 9 to 12) and displaces the granite located to the north in the hanging wall above the main $P_1 \times P_2$ anticline located in the footwall. The carbonate embayments north of the main anticline and the associated mineralization are thus uplifted and thrust southward. This main F_2 fault zone has a dip-slip that is at least hectometric. Another important F_2 fault zone may be inferred from drillings in the lower part of the Véronique deposit (Fig. 10). Many other F_2

faults are known in many parts of the La Fourque stock and play a role in the details of the shape of the intrusion and in the distribution of skarns and later hydrothermal mineralization.

4. Some very late wrench faults trending $N 30^\circ E$ and $N 160^\circ E$ may offset previous faults and orebodies.

Types of ore and distribution of orebodies

The Salau deposit comprises two main parts: the outcropping Bois d'Anglade deposit to the east and the blind Véronique deposit to the west (Figs. 9 to 13). The two parts of the deposit are separated by granodiorite apophysis A (Figs. 9 and 14). Each part of the deposit includes a series of orebodies showing various types of ore. Observed relations between geologic setting and ore mineralogy allow three main types to be defined (Fonteilles et al., 1988):

1. Type 1 is the oldest economic mineralization known in the mine. It consists of quartz + scheelite ($0.7-2.5\% \text{WO}_3$, avg 1%) + arsenopyrite \pm pyrrhotite in F_0 mylonites. This type of ore is only known in the Véronique Southeast orebody (Fig. 13), south of the Véronique fault, where it has been exploited between the 1,430 and 1,486 levels.

2. Type 2 consists of massive pyrrhotite + quartz richly mineralized in scheelite without any trace of crushing at sample scale, commonly containing centimetric to pluridecimetric lenses of contorted graphitic limestones and skarns. This type of ore is located in the graphitic marbles at the intersection of an F_1 fault with the intrusive contact. Part of the type 2 ore is located inside the granodiorite along the F_1 fault. Type 2 ore forms the Formation Sud orebody of the southern part of the Bois d'Anglade embayment and the Véronique Southeast orebody. These orebodies are offset and reworked by the F_2 faults (Figs. 10 and 12). In the part where they are crosscut by F_2 faults they are very irregular in shape and have less economic interest. Prior to the F_2 faulting, the Véronique Southeast orebody was a more than 300-m-high, very homogeneous column, dipping $70^\circ W$. Its lateral extension is nearly 50 m. Eastward, this structure closes down abruptly where the F_1 fault enters apophysis A; westward, the orebody becomes discontinuous and the grade decreases progressively.

3. Type 3 consists of pyrrhotite \pm scheelite \pm skarn residues mostly developed at the expense of skarns along the flanks and the bottom of embayment structures and occurs in a comblike structure normal to the intrusive contact. The Bois d'Anglade embayment is a synform of calc-silicate hornfels surrounded by the granodiorite but open to the east (Figs. 11 and 12). Type 3 ore mostly developed along the northern contact (Formation Nord orebody) and to the west

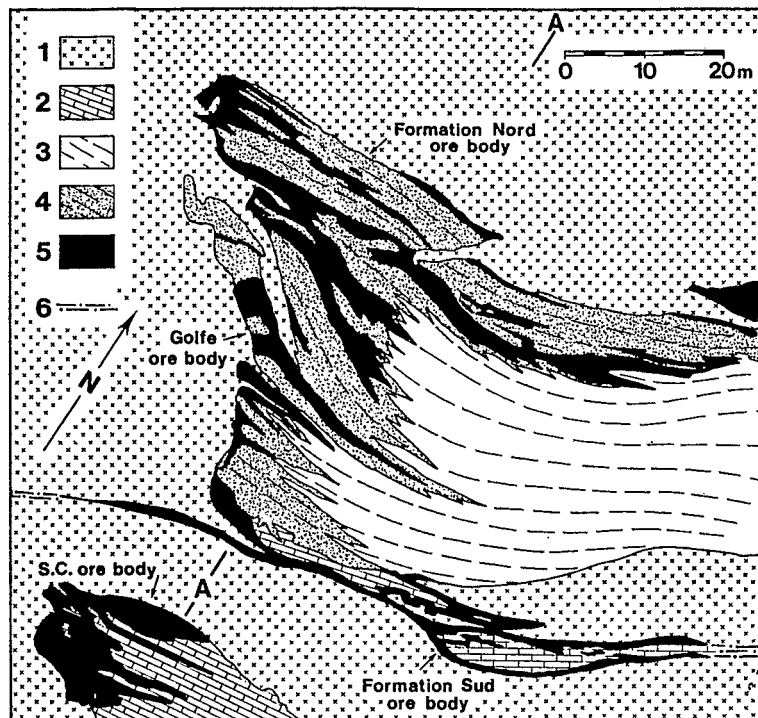


FIG. 11. Map of the 1452 level of the Bois d'Anglade deposit (modified from J. Faure, S.M.A. unpub. documents). 1 = intrusive rocks, 2 = marbles, 3 = calc-silicate hornfels, 4 = calc-silicate hornfels skarns, 5 = ore, 6 = F_2 fault. AA = cross section of the Bois d'Anglade deposit.

and at depth (Golfe orebody). Farther south, the S.C. orebody occurs in a similar structure but is of lesser importance. In the western part of the mine, the Véronique West upper orebody appears to be a structure similar and symmetrical to the Bois d'Anglade embayment but smaller and opened to the west. The Véronique West lower orebody is the same orebody offset by the main F_2 reverse fault (Fig. 14). Its western and lowest extension is unknown. The deepest known drill hole intersection is at a 1,080-m elevation.

With the possible exceptions of zones V and VI, which are minor orebodies located in the upper part of the deposit and of the Christine showing, all the known orebodies are located in an aureole around the parabolically shaped barren area formed by apophysis A (Fig. 14). This distribution may be interpreted as being linked to an F_1 fault intersecting the granodiorite apophysis A. This fault dies away within the limestones. Type 2 ore has thus only developed in the immediate neighborhood of the points where this fault emerges from the granodiorite (i.e., in an aureole around apophysis A) by the transformation of skarn at the contact between the granite and the graphitic limestone. According to Kaelin (1982), fault F_1 was thus the channel through which the fluids responsible for the mineralization arrived.

This is consistent with the richness of this mineralization and the almost complete transformation of skarn into massive pyrrhotite and scheelite ore. The granodiorite immediately adjacent to the orebodies appears to have played only a passive role and remained mostly barren. The source region was lower along F_1 fault.

Type 3 ore appears to be the result of an "oil-stain" extension of the mineralization where the fluid was able to reach and penetrate the calc-silicate hornfels, which are clearly favorable to circulation and transformation. This oil-stain development, by infiltration, is consistent with the ragged aureole formed by the type 3 orebodies around the most proximal and regular type 2 orebodies. Zones V and VI could be slightly more remote extensions of these type 3 discontinuous mineralizations.

Outside the mine itself, another structure similar to the F_1 fault is suspected on the northern side of the La Fourque stock. The two known groups of occurrences to the northeast and the northwest on either side of the La Fourque stock and the Christine showing (Figs. 2 and 14) could correspond to the intersection of this F_1 plane with the edges of the granodiorite. The Christine showing is a blind embayment structure (intersected only by drilling) opening westward between 1,160- and 1,230-m elevations includ-

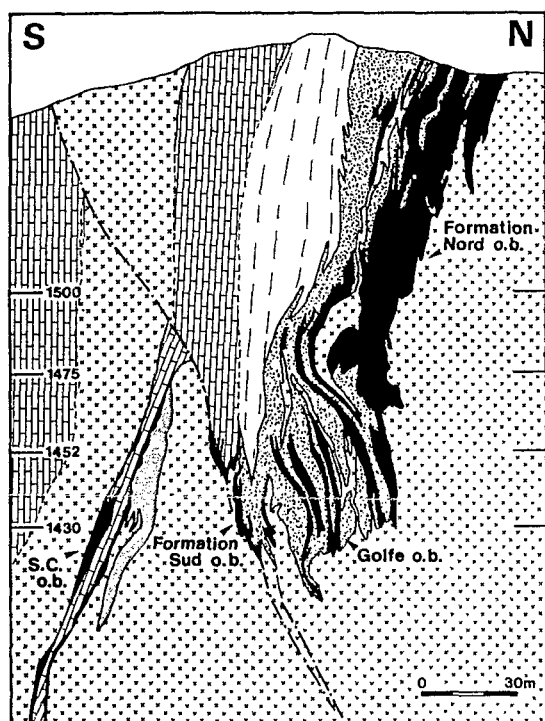


FIG. 12. Vertical north-south cross section of the Bois d'Anglade orebodies (modified from L. Nansot, Société Minière d'Anglade unpub. documents). Symbols as in Figure 11. Location of the cross section is given in Figures 9 and 11.

ing some very rich (8% on 0.6 m) type 2 ore. It could be a promising target.

Petrography and Geochemistry of the Intrusive Rocks

Petrography

The La Fourque granodiorite is a composite stock (Fonteilles and Machairas, 1968; Soler, 1977; Kaelin,

1982; Rimbault and Kaelin, 1987). The main part is a medium-grained (0.5–2 mm) granodiorite, generally equigranular but locally porphyritic. The apical part shows a rather special texture characterized by idiomorphic plagioclase and biotite surrounded by large xenomorphic and poikilitic quartz crystals.

The mineralogy of those rocks includes quartz—locally with an idiomorphic tendency, idiomorphic plagioclase with overall normal zoning from An_{55} to An_{20} with a few reversals, microcline, reddish-brown biotite, and accessory ilmenite, apatite, zircon, and allanite. Almandine garnet occurs in one granite variety (garnet-bearing granodiorite; analysis 348, Table 2) and in very rare rocks which may be interpreted as biotite-garnet cumulates (analysis 351, Table 2). Hornblende has been found in a local very dark variety (analysis 2, Table 2), which may be interpreted as a cumulate of an earlier, less evolved stage.

Some parts of the La Fourque stock are crowded with decimetric oval inclusions of more or less fine-grained diorite and granodiorite. Rare small angular inclusions of pelitic host rocks are known near the margins of the stock.

In the vicinity of skarns and orebodies and along fault planes the La Fourque stock has been modified by skarn-forming and various hydrothermal processes, including greisenization, albitization, and late-stage alteration. These will be discussed below together with the description of skarns and mineralization.

The sills and dikes have a mineralogy similar to that of the main intrusion, usually with a finer grained texture; some are porphyritic (Zandvliet, 1960). In composition, the sills are more mafic on average than the La Fourque stock and the dikes. They include amphibole-biotite quartz diorites, with plagioclase cores reaching An_{80} in some cases.

Geochemistry

The La Fourque stock includes various granitic rock types (Table 2). They are rather mafic types (3%

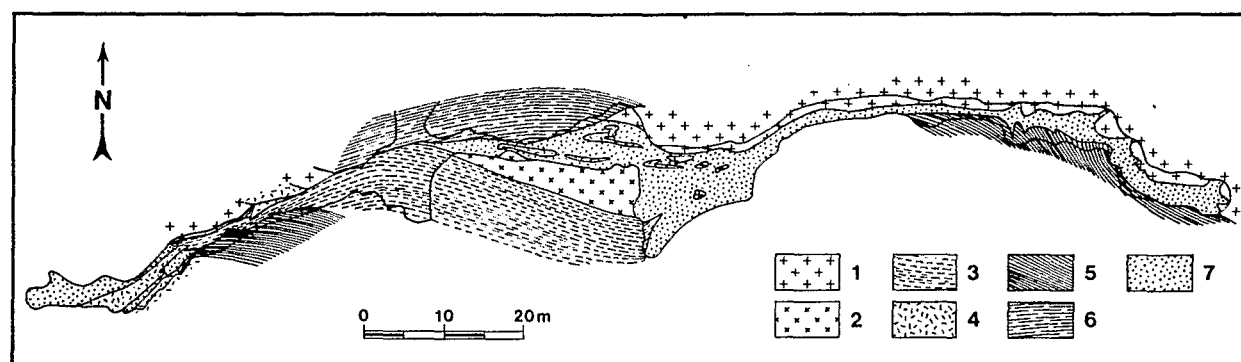


FIG. 13. Location of the type 1 ore (map of the DV 1470 level, from Kaelin, 1982). 1 = granodiorite, 2 = albitized granodiorite, 3 = silicified and mineralized mylonites (F_0 and type 1 ore), 4 = marble, 5 = calc silicate hornfels, 6 = calc-silicate hornfels skarns, 7 = massive pyrrhotite (partly mineralized).

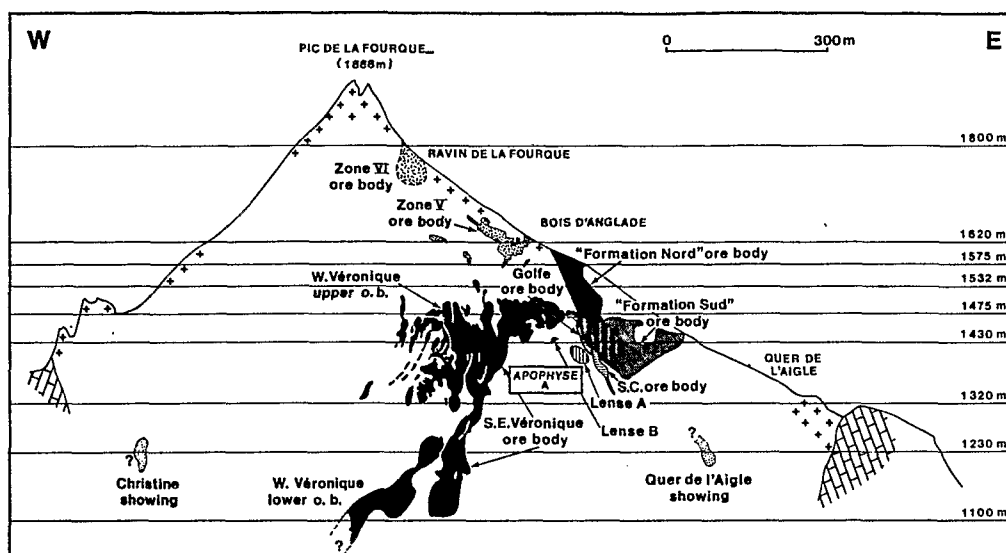


FIG. 14. Distribution of the orebodies around granodioritic apophysis A projected onto a vertical east-west plane (modified from L. Nansot, Société Minière d'Anglade unpub. documents).

> MgO > 0.50%) compared with other Pyrenean granites.

Two trends have been identified by Soler (1977) and Kaelin (1982); within each trend the representative points on the various diagrams are grouped in clusters which seem to represent distinct magma batches.

Trend I, developed in the outer parts of the stock in the vicinity of the mine, includes two main rock types: minor quartz diorites (sample 903) and granites (samples 348, 912, 914). It is characterized by high Fe_2O_3 and low K_2O contents.

Trend II, observed in the central part of the stock and as crosscutting dikelets through the outer part, includes three rock types: minor diorites (sample 901), mostly garnet-bearing granodiorites (sample 938), and minor monzonitic granites (sample 937). The medium-grained porphyritic rocks belong to this family. Trend II is richer than trend I in K_2O (Fig. 15) and Fe_2O_3 (Fig. 16) for a similar MgO content. Evolution of TiO_2 content also is different for the two trends (Fig. 17) and trend II appears slightly richer in Zr than trend I (Fig. 18).

Trend I is exceptional in the Pyrenees. Other Pyrenean Hercynian granites (Fig. 1), including, for example, the Querigut (Letierrier, 1972), Mont Louis, and Costabonne (Autran et al., 1970) massifs, show trends similar to the La Fourque trend II. Notwithstanding its iron-rich trend similar to the La Fourque trend I, the Batère massif (Autran et al., 1970) is as rich in K_2O as the normal Pyrenean granites.

In the Variscan belt of southern France, K_2O -poor granites similar to the La Fourque trend I are known

only in Corsica (Cocherie, 1985) where they are also associated with larger amounts of K_2O -normal types. The association of both types (low K and normal K granites) is also common in the western coast of North and South America (Peninsular Range, Moore, 1959; Guichon in Canada and Santa Rosa in southern Peru, Johan et al., 1980) and in the Jurassic Daebö series of South Korea (Iiyama and Fonteilles, 1981).

Contact Metamorphism

The first effect of contact metamorphism was the development of biotite in rocks of favorable compositions at a distance on the map of at most 900 m from the contact of the La Fourque stock. A more intense contact effect results in a systematic development of a calc-silicate assemblage at the expense of the Barrégiennes, in a narrow zone of 50 m mean width (always less than 100 m) near the contact. This calc-silicate assemblage consists of: in marbles—calcite, graphite, quartz, calcic plagioclase, amphibole, clinopyroxene, clinozoisite, and biotite; and in Barrégiennes—calcite, quartz, clinozoisite (pistacite₂₅₋₆₅, with MnO content < 0.4%), salite (hedenbergite₂₀₋₄₀, with johannsenite content < 3 mole %), calc-aluminous garnet (grossular₈₃₋₉₄ andradite₁₁₋₅ almandine_{4.3-0.7} spessartite_{<1} pyrite_{2.3} with fluorine content commonly reaching 0.2%), vesuvianite (commonly zoned with 2.4–5.7% FeO, 0.8–2.5% MgO, 0.15% MnO, and 0.6–3.6% TiO_2), rare microcline, sphene (with 3% Al_2O_3), apatite, and graphite; wollastonite is rare. All these minerals occur in a variety of associations depending on the original com-

TABLE 2. Selected Whole-Rock Analyses of the La Fourque Stock and Associated Dikes

Sample no.	Low K early suite					Normal K suite				Dikes	
	903	348	912	914	2	351	901	938	937	923G	928A
SiO ₂	66.84	71.38	70.93	71.19	53.73	54.91	62.43	63.55	69.96	70.58	76.64
Al ₂ O ₃	16.65	13.31	15.33	14.59	18.22	17.07	16.05	17.12	15.39	15.61	13.75
Fe ₂ O _{3total}	3.83	2.13	2.24	2.05	8.45	10.00	6.39	5.36	2.42	2.42	0.42
MnO	0.08	0.05	0.03	0.02	0.15	0.22	0.17	0.06	0.02	0.01	tr.
MgO	1.43	0.55	0.55	0.54	5.43	4.14	2.63	1.22	0.55	0.71	0.14
CaO	3.80	4.09	1.63	1.76	7.66	2.66	3.48	3.91	2.35	1.66	0.64
Na ₂ O	3.72	4.01	4.12	3.62	1.76	1.87	3.40	2.97	2.96	3.10	3.10
K ₂ O	1.65	2.55	3.27	2.95	1.76	2.18	1.61	3.01	3.74	4.05	3.62
TiO ₂	0.45	0.31	0.32	0.35	0.97	0.90	0.70	0.51	0.17	0.22	0.05
P ₂ O ₅	0.17	0.11	0.09	0.14		0.28	0.25	0.15	0.08	0.05	0.18
L.O.I.	1.82	0.52	1.53	1.28	2.45	3.77	2.10	1.03	0.82	1.50	1.73
Total	100.44	99.03	100.07	99.57	100.58	98.12	99.21	98.98	98.56	100.16	100.54
Ba								546	499		291
Sr	176	196	270	130		507	278	218	186	287	83
Rb	98	67	126	131		124	72	126	149	132	123
Zr	159	132	138	145		291	186	175	118	102	30
U								2.0	2.1		2.3
Th								8.9	12.7		0.4
Y	18.4	17.8	15.2	17.0		62.2	33.0	21.9	13.5	15.9	13.3
W								0.3	0.3		1.4
La								32.0	38.5		1.2
Ce								56.0	72.0		2.0
Sm								5.7	6.7		
Eu								1.5	1.3		0.2
Tb								0.5	0.3		0.2
Yb								1.3	0.3		0.4

Major elements (wt %) analyzed by XRF (Laboratoire de Géologie, Ecole des Mines de Saint-Etienne, France; analysts J. J. Gruffat and L. Raimbault)

Trace elements (ppm) analyzed by XRF (Laboratoire de Géologie, Ecole des Mines de Saint-Etienne, France; analysts J. J. Gruffat and L. Raimbault), except Ba, U, Th, W, and REE for samples 937 and 938 by INAA (Laboratoire Pierre Sue, Centre d'Etudes Nucléaires de Saclay, France; analyst L. Raimbault)

position of the bands (Fonteilles and Machairas, 1968; Soler, 1977), the effects of chemical diffusion between carbonate and pelitic bands (Zahm, 1987a, b), and the metamorphic grade.

Geochemical data (Zahm, 1987a and b) show that this metamorphism has been nearly isochemical, except as usual for CO₂ and H₂O. However, some of the calc-silicate hornfels show a significant depletion in K₂O and Na₂O (Fig. 19) and practically all present a clear decrease in Rb (Fig. 20).

Metasomatism

At Salau, skarns are developed in marbles and calc-silicate hornfels (exoskarns) and in intrusive rocks (endoskarns). The exoskarns are restricted to an almost 30-m-thick zone of carbonate host rocks at the contact with the granodiorite. The endoskarns are restricted to the rim of the granodiorite and to thin granodiorite dikelets that cut the carbonate host rocks. Three stages may be distinguished during skarn formation: a first metasomatic stage with the development of the bulk of the exo- and endoskarns, a second

stage of partial hydration of primary skarn minerals, and a third stage characterized by the development of a late garnet at the expense of the primary skarns and the other silicate rocks.

Primary skarns

Exoskarns: Primary skarns developed on the marbles (henceforth termed marble skarns) represent 10 percent or less of the exoskarns. Most of them are veinlike skarns with clear crosscutting relations with the banding of the graphitic marble. They are commonly thin (from less than 1 cm to 0.5 m), and where later deformation or hydrothermal alteration have not blurred the relations, commonly show very clear zonation with very sharp metasomatic fronts. Three types of zonation have been recognized (see in Table 3 the composition of the different zones). The complete type A zonation is rare (Soler, 1977); type B is uncommon, and the usual case is type C (Fonteilles and Machairas, 1968; Soler, 1977). The wollastonite external zone IIIA has been observed only in a very few cases (Zahm, 1987a, b), but a very thin external

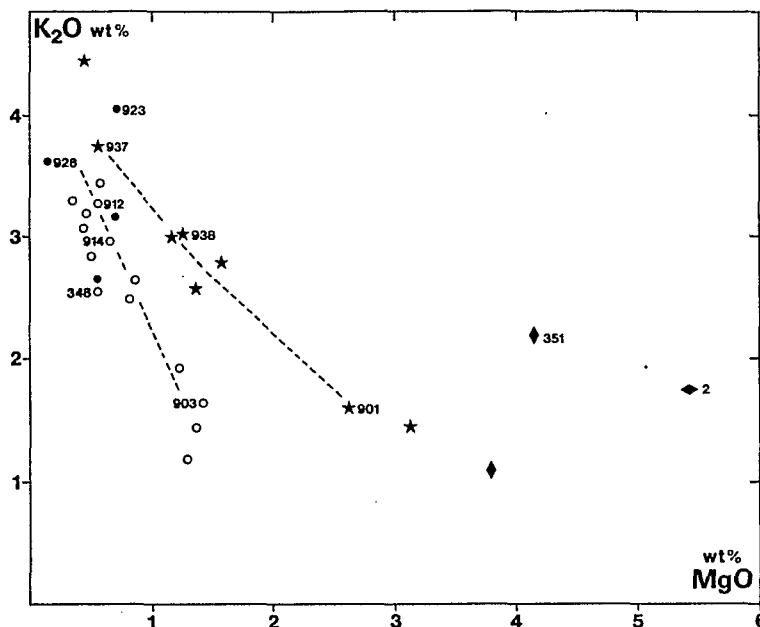


FIG. 15. K_2O vs. MgO diagram for samples from the La Fourque intrusive stock and associated dikes. Symbols: open circles = quartz diorites to granites (trend I), black stars = diorites to monzonitic granites (trend II), black diamonds = cumulates (trend II), black circles = dikes.

zone of quartz + calcite (retromorphosis of wollastonite) is present at various places. Types A, B, and C may be considered as a spatial succession along the trace of veins—type A near the source and type C downstream (Figs. 21 and 22). The closing of the inner zones and ultimately of the outer hedenbergitic zone in the marble (Fig. 22) has been observed at many places. Relict hedenbergite crystals in some cases are observed enclosed in the garnet; they can be considered as witnesses of the downstream advance of the fronts during the metasomatic process (Korzhinskii, 1969; Fonteilles, 1979). Zone I of type A skarn represents an endoskarn developed on a granodioritic dikelet as discussed below. Where the garnet (grosular—zone II) is present, the thickness ratio of garnet and pyroxene (hedenbergite—zone III) zones is 1/10 to 1/20. The bleached marble zone IV is narrow in most cases (<1 cm) and its thickness is not related to that of the pyroxene zone. The plastic flow deformation and disharmonic folding of the marbles mentioned above commonly are associated with boudinage of the skarn veins (Fig. 23).

The primary skarns developed on the calc-silicate hornfels (henceforth noted calc-silicate hornfels skarns) represent the bulk of the exoskarns. They are massive or veinlike, with very irregular shapes. Their contact with the calc-silicate hornfels shows generally crosscutting relations with the original banding, which is preserved inside the skarn as alternating bands of garnet and pyroxene. In the veinlike skarn, a zonation

similar to that of type B skarn mentioned above can be observed in some places (Zahm, 1987a).

The development of these skarns in many cases has been controlled by the banding of the calc-silicate hornfels, as shown by the comblike structure of the contact at small scale (Fig. 24). The skarns which developed at the contact with the granodiorite are thicker where the banding of the calc-silicate hornfels makes a large angle with the contact (Fig. 12). In this case the skarn thickness perpendicular to the contact may reach some 20 m. The vein skarns and the skarns developed where the contact of the granodiorite is parallel to the banding of the calc-silicate hornfels are much thinner (10–50 cm).

An intermediate zone of light-colored calc-silicate hornfels skarn, the thickness of which may reach several meters, generally separates this dark, mostly hedenbergitic, skarn from the calc-silicate hornfels. The limit between the dark calc-silicate hornfels skarn and the light-colored calc-silicate hornfels skarn is sharp; the contact between the latter and the calc-silicate hornfels is comparatively sharp, but when this contact is not directly observed, it may be difficult to distinguish the light-colored skarn from the calc-silicate hornfels without chemical information.

At some places in the mine, one can observe the continuity between the dark calc-silicate hornfels skarns and the skarns developed in the adjacent marbles (Fig. 24), indicating that both these skarns developed through the action of the same metasomatic

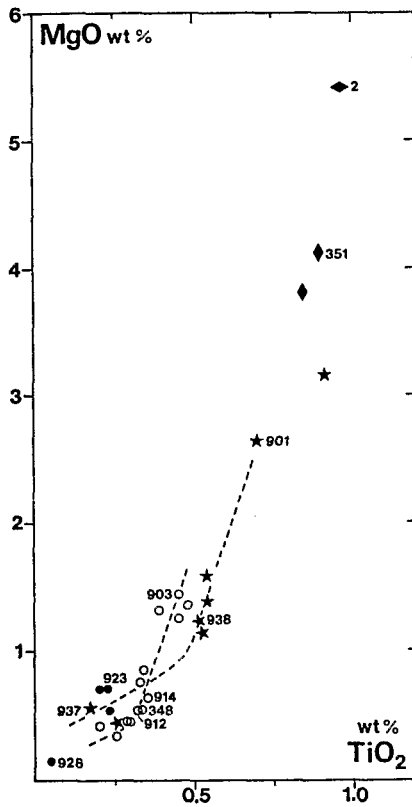


FIG. 16. Fe_2O_3 vs. MgO diagram for samples from the La Fourque intrusive stock and associated dikes. Symbols as in Figure 15.

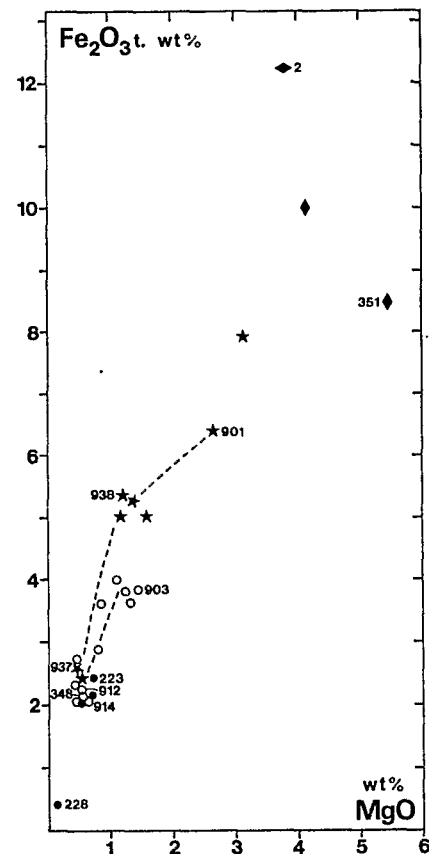


FIG. 17. MgO vs. TiO_2 diagram for samples from the La Fourque intrusive stock and associated dikes. Symbols as in Figure 15.

fluids. Morphological differences discussed here, and mineralogical and petrographical differences discussed below, must be related to the chemical contrast between the marbles and calc-silicate hornfels.

The pyroxene of the marble skarns is hedenbergite with 0 to 12 percent diopside and 2 to 10 percent johannsenite components (Fig. 25C). Al_2O_3 , TiO_2 , and Na_2O contents are negligible. In these skarns, the hedenbergite appears as millimetric to centimetric elongated crystals with an idiomorphic tendency, in a criss-cross texture preserving important intergranular spaces. Occasionally this pyroxene presents a comb texture with parallel or fan-shaped sheaves of pluricentimetric (up to 3 cm) elongated crystals. Scheelite is commonly associated with pyroxene; it appears as rounded crystals some 0.5 mm or less in diameter. The contemporaneity of both minerals is suggested by intergrowth textures between scheelite and pyroxene. In the zoned marble skarns (types A or B), primary scheelite appears only in the outer half of the hedenbergitic zone III (Soler, 1977). This is an additional argument in favor of primary scheelite being contemporaneous with skarn formation. WO_3 content in the skarn is in the range 0.1 to 0.4 percent. Where the skarn has not been transformed by late

hydrothermal processes, the intergranular spaces are filled with quartz, calcite, and/or pyrrhotite and scheelite. The pyroxene from the calc-silicate hornfels

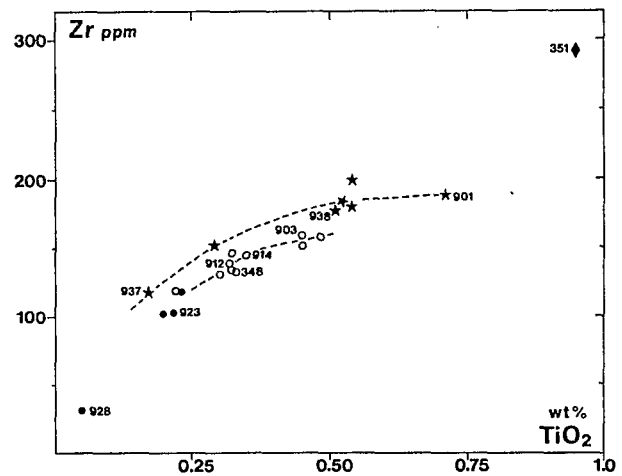


FIG. 18. Zr vs. TiO_2 diagram for samples from the La Fourque intrusive stock and associated dikes. Symbols as in Figure 15.

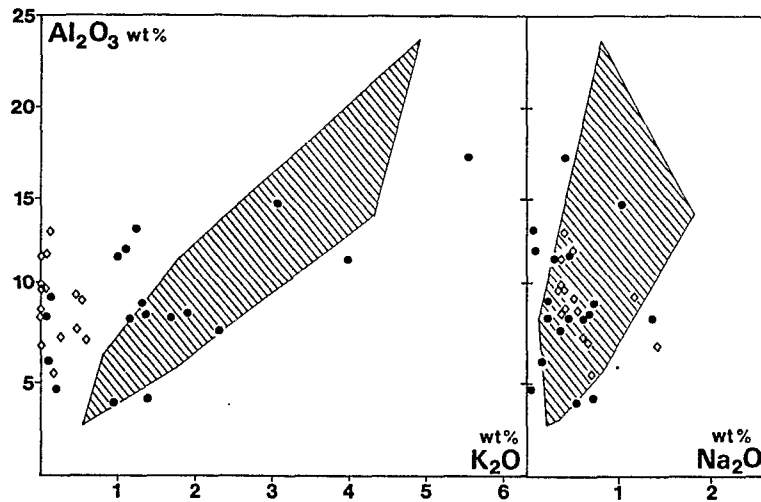


FIG. 19. K_2O and Na_2O vs. Al_2O_3 diagram for Barrégiennes (stippled field), calc-silicate hornfels (black circles), and light-colored calc-silicate hornfels skarns (open diamonds). Data from Zahm (1987a).

skarns shows the complete range of composition linking the fields of the calc-silicate hornfels pyroxene (see above) to that of the pyroxene from the marble skarns (Fig. 25B). The pyroxene composition outside the field of the calc-silicate hornfels is characterized by a distinctly higher johannsenite component (2–10%) similar to that of the pyroxene from the marble skarns. In the calc-silicate hornfels skarns, the pyroxene appears as millimetric, equidimensional crystals, coarser grained than the pyroxene from the calc-silicate hornfels.

The garnet from zone II of the marble skarns is macroscopically pale red and commonly anisotropic

in thin sections. Anisotropy is variable and may occur in crystallographic zones or in more or less regular sectors. The garnet is grossularitic with 72 to 82 percent grossular, 11 to 15 percent andradite, and 6 to 19 percent almandine + spessartite components (Figs. 26C and 27). Its fluorine content commonly is 0.6 percent or more (up to 1.20%). The MgO content is characteristically lower than 0.03 percent. This garnet, in millimetric to centimetric crystals, shows some idiomorphic tendency with a polygonal texture preserving very few intergranular spaces. The garnet composition is the same in marble skarns of types A and B. Primary scheelite has never been observed in

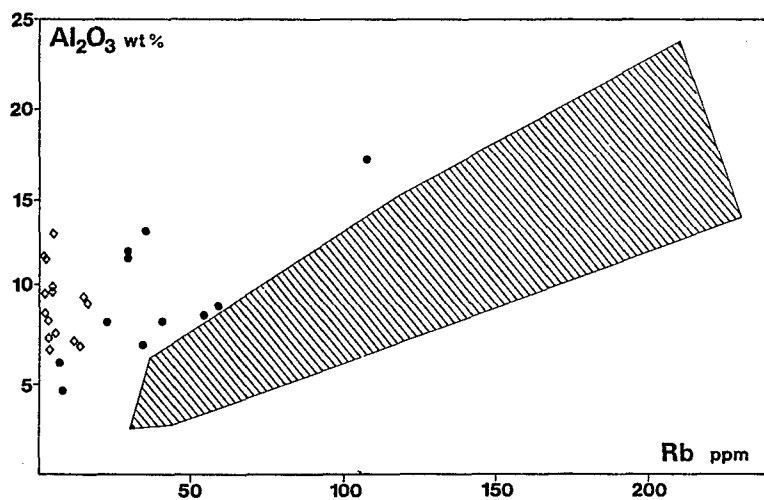


FIG. 20. Rb vs. Al_2O_3 diagram for the Barrégiennes, the calc-silicate hornfels, and the light-colored calc-silicate hornfels skarns. Data from Zahm (1987a). Symbols as in Figure 19.

TABLE 3. Zoning of Skarns Developed in the Marbles

Type A (rare)	II	III	IIIA	IV	
I Epidote, amphibole, sphene-apatite, allanite	Grossular garnet	Hedenbergite	(Wollastonite)	Bleached marble	Graphitic marble
Endoskarn	← Exoskarn →				
Type B (uncommon)	Grossular garnet	Hedenbergite	(Wollastonite)	Bleached marble	Graphitic marble
Type C (very common)		Hedenbergite	(Wollastonite)	Bleached marble	Graphitic marble

association with this garnet. Calc-silicate hornfels skarn garnet shows a tendency to higher grossular and andradite and lower almandine contents than garnet from the marble skarns (Fig. 26B and C). However, compositional fields of primary garnets from the two skarns overlap widely.

In all the exoskarns, a large addition of silica, iron, and manganese has taken place. This is obvious for the marble skarns and very clear in the case of the calc-silicate hornfels skarns from the minerals or whole-rock chemical analyses. The light-colored calc-silicate hornfels skarns show addition of these elements in smaller amounts and appear to have an intermediate composition between calc-silicate hornfels and dark skarns. In the marble skarns, a large addition of aluminum occurs in the innermost garnet zone. In the pyroxene zone of the marble skarns no aluminum was introduced. In the calc-silicate hornfels skarns no addition of aluminum has been observed, except in relation to the development of garnet veins. The MgO contents of the marble skarns are in every case very low (<2%). In the dark skarns MgO contents are in the range of 1.5 to 3 percent, which is the same as the range of MgO contents of the calc-silicate hornfels

and the Barrégiennes. However, enrichment in MgO (up to 8%) is the most distinctive characteristic of the light-colored skarns (Fig. 28). The P_2O_5 contents in marble skarns and dark skarns are low (0.05–0.15%) and are similar to the P_2O_5 contents of the Barrégiennes and the calc-silicate hornfels. Only in the light-colored skarns, is some P_2O_5 enrichment (up to 0.5%) observed.

Endoskarns: Endoskarns are much less developed than exoskarns. They are discontinuous and observed only at a few places at the contact between the granodiorite and the carbonate host rock; the thin granodiorite dikes that cut this host rock are generally transformed into endoskarn and constitute the central (I) zone of the A type of marble skarns. The thickness of the endoskarn, perpendicular to the contact, does not exceed a few decimeters.

The characteristic assemblage of these endoskarns is epidote + amphibole + sphene. Allanite commonly constitutes the core of the epidote crystals and apatite is a common, in some cases an abundant, accessory mineral. Quartz and calcite may be associated with the amphibole. Hypidiomorphic epidote (pistacite₆₀₋₇₀ clinozoisite₄₀₋₃₀) is by far the most abundant mineral. The fibrous amphibole is a ferroactinolite with MnO contents near 1.0 percent. On the basis of textural observations, it has been suggested (Soler, 1977) that both epidote and amphibole are secondary minerals developed at the expense of a primary assemblage of calcic plagioclase + pyroxene which formed by reaction with the carbonate host rock, possibly at the magmatic stage. This hypothesis is in agreement with observations at contacts between granitoids and carbonate rocks in many other skarns (e.g., Fonteilles, 1962); however, no actual preserved plagioclase + pyroxene association has ever been observed in the Salau mine.

Chemical data on whole rocks and minerals show that endoskarns are not only very rich in calcium but also in iron and manganese compared with adjacent untransformed granodiorite. This constitutes evidence of chemical inputs which cannot be the result of as-

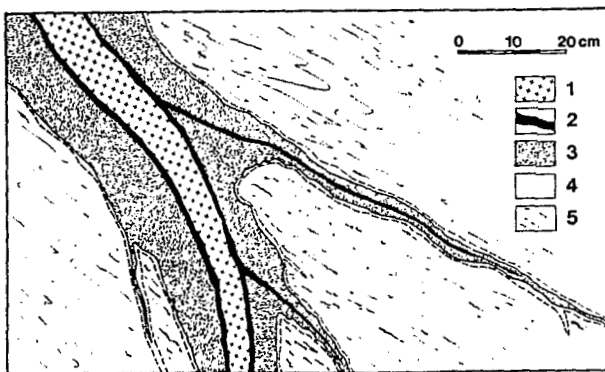


FIG. 21. An example of zones of marble skarns (from Soler, 1977). 1 = internal endoskarn zone, 2 = garnet, 3 = hedenbergite (\pm scheelite), 4 = bleached marble, 5 = graphitic marble.

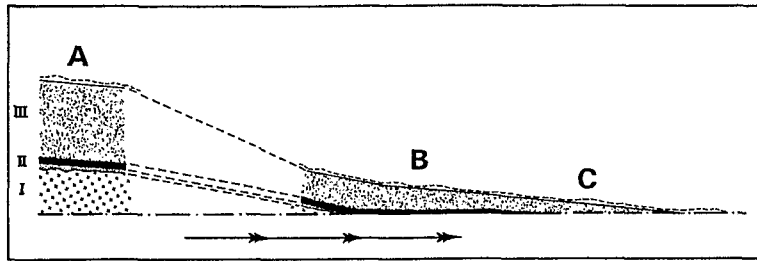


FIG. 22. The zonation of the marble skarns (see Table 3). Symbols as in Figure 21. Discussion in text.

similation of carbonates or diffusion from the carbonated host rock which has low Fe and Mn contents. These inputs (Fe, Mn, Ca²⁺) are probably related to the stage of infiltration metasomatism responsible for the formation of the exoskarns.

Early hydration of skarn minerals

At many places in the mine, the primary assemblages discussed above were transformed into hydrous calc-silicate assemblages prior to the development of the late-stage garnet skarns (see below and Fig. 29) and later hydrothermal processes. The early garnet is replaced by an epidote + calcite + quartz assemblage. This transformation is very irregular. It generally occurs in veinlets but may be locally massive. It is possible that at least part of the observed transformation of the hedenbergitic pyroxene into a ferri-ferrous amphibole of the actinolite-tremolite series has occurred at this stage.

The compositions of the primary garnet and the associated epidote suggest that this stage of transformation of primary skarn assemblages does not require any chemical input except for water and carbon dioxide.

Late-stage garnet skarns

This stage is mainly represented by a macroscopically red garnet, distinctly colored and isotropic in thin sections. This garnet is commonly accompanied

by masses of black quartz. As associated minerals, blue-green hornblende is not rare and scapolite (meionite) has been observed in one place.

Late garnet skarns are more abundant in the Veronique orebodies than in the Bois d'Anglade. They developed in silicate rocks: either in granodiorite, endoskarns, or marble and calc-silicate hornfels skarns of the early stage. In thin sections, late garnet clearly postdates hydrous calc-silicate-bearing assemblages developed in the early skarns. Whatever the type of involved silicate rock, the late garnet develops preferentially in silicate rock at the contact with the carbonate host rock (Fig. 29). It appears as veins, vugs, or masses. The thickness of the veins is centimetric or less and the dark quartz is commonly observed along the borders of the veins. Where the veins enter the marble host rock, they grade into indistinct recrystallization veins (Fig. 29). In the calc-silicate hornfels skarns, the late-stage garnet develops mostly as irregular decimetric masses guided by the banding.

When compared with the garnet from the marble and calc-silicate hornfels skarns, the late-stage garnet has a broad range of compositions, lower grossular (45–70%) and andradite (3–10%) contents, and higher almandine (10–24%, exceptionally between 30 and 40%) and spessartite (8–24%, exceptionally as low as 3%) contents (Figs. 26D and 27). Its fluorine content (0–0.4%) is characteristically lower than that

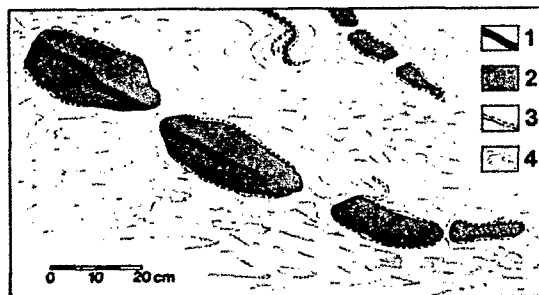


FIG. 23. Boudinage of the marble skarns. 1 = garnet, 2 = hedenbergite, 3 = bleached marble, 4 = graphitic marble.

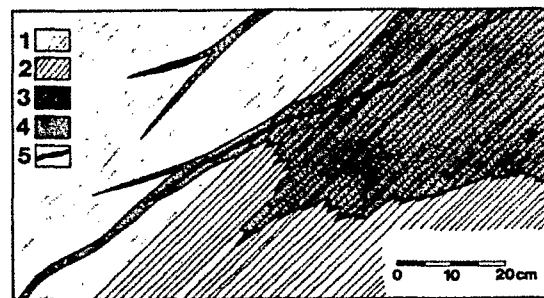


FIG. 24. Relations between marble skarns and calc-silicate hornfels skarns (from Soler, 1977). 1 = graphitic marble, 2 = calc-silicate hornfels, 3 = calc-silicate hornfels skarn, 4 = hedenbergitic marble skarn, 5 = primary skarn garnet.

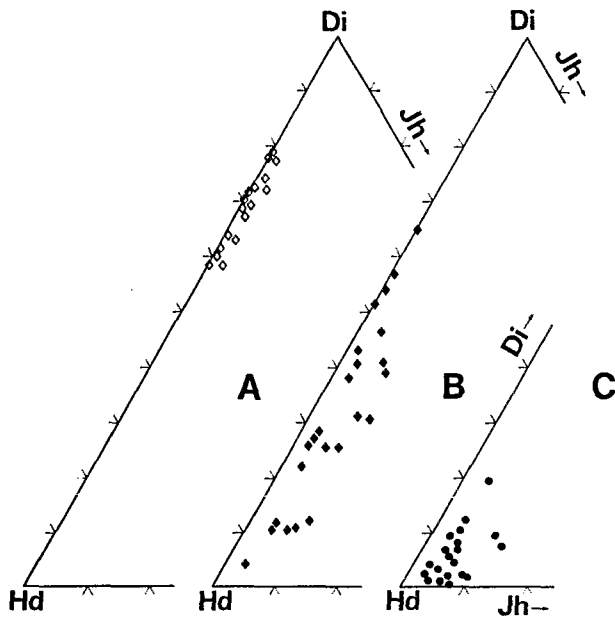


FIG. 25. Composition of pyroxenes (in mole %). A. In calc-silicate hornfels. B. In calc-silicate hornfels skarns. C. In marble skarns. Di = diopside, Hd = hedenbergite, Jh = johannsenite. Electron microprobe data from Soler (1977) and Zahm (1987a).

of the primary marble or calc-silicate hornfels skarn garnet. In a few cases, late-stage garnet shows a continuous range of compositions from that of a primary garnet to a typical high almandine + spessartite type (Zahm, 1987a, b). In most cases, however, no intermediate composition is found and when late-stage garnet veins cut a primary marble or calc-silicate hornfels skarn garnet zone (more or less epidotized), one finds in some cases zoned crystals with a relict

primary garnet core and late garnet rims (Kaelin, 1979). Such garnet has been described in numerous tungsten-bearing skarn deposits (e.g., Shimazaki, 1977; Einaudi et al., 1981; Newberry, 1983; Fonteilles and Garcia, 1985).

Late Hydrothermal Processes and Mineralization

Most of the metasomatic rocks described in the last section and part of the granodiorite underwent intense late hydrothermal alteration. Geologic distribution in the mine supplemented by microscopic observations permits the distinguishing of various stages and establishes their relative chronology.

Greisen and arsenopyrite stage

Greisen development is scarce and restricted to small veins in the granodiorite. The assemblage is quartz + muscovite ± tourmaline. Arsenopyrite occurs in some of these veins with rare wolframite and in altered (silicified) granodiorite (Fonteilles and Machairas, 1968; Soler, 1977). A local development of arsenopyrite in centimetric to decimetric clusters also is observed in the hedenbergite skarn.

Partial albitization of the feldspars has been noted at various places in the stock. Biotite remains stable at this stage. Exceptionally, this transformation may produce true albitites with the disappearance of quartz. Detailed study of this phenomenon is not available and its relative chronology is not clearly established.

Pyrrhotite and scheelite stage

This second stage corresponds to the massive development of pyrrhotite and scheelite at the expense of the skarns and in some cases of the granodiorite.

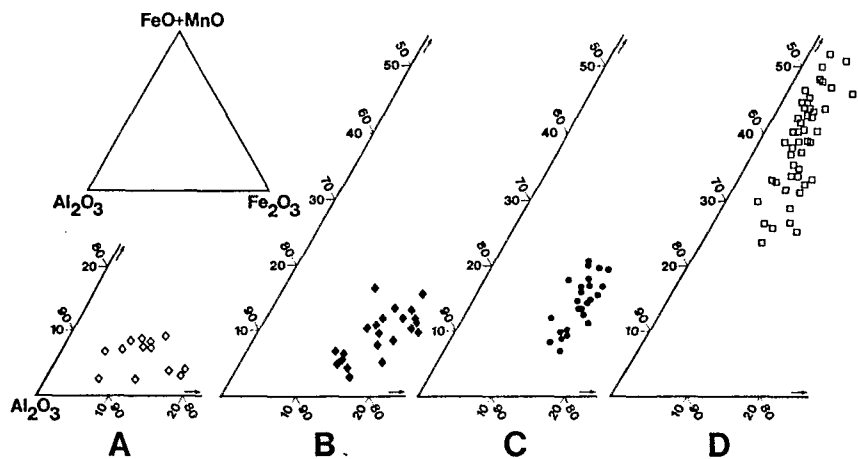


FIG. 26. Composition of garnets (in mole %). A. In calc-silicate hornfels. B and C. Primary skarn garnet (B, in calc-silicate hornfels skarns; C, in marble skarns). D. Late skarn garnet. Electron microprobe data from Soler (1977), Kaelin (1979), and Zahm (1987a).

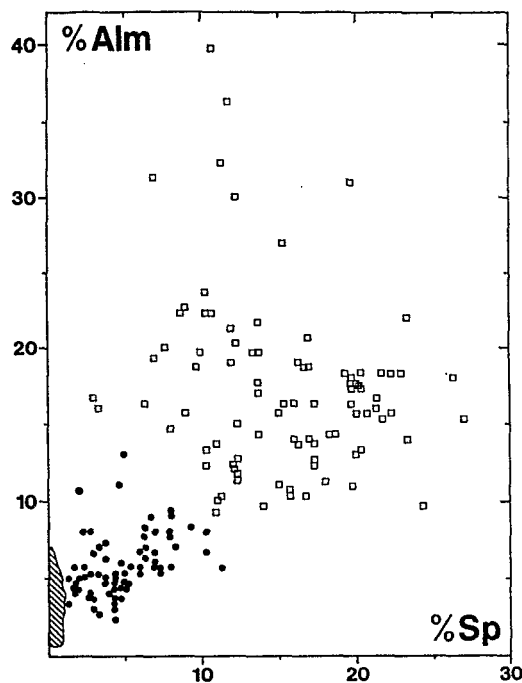


FIG. 27. Composition of garnets (in mole %). Symbols: black circles = garnet from primary marble and calc-silicate hornfels skarns, open squares = late garnet, stippled area = field of composition of garnet from calc-silicate hornfels. Electron microprobe data from Soler (1977), Kaelin (1979), and Zahm (1987a).

Mineral assemblages of this stage depend on the nature of the original rock.

In skarns, the typical assemblage is pyrrhotite + scheelite \pm amphibole (with relict hedenbergite) + epidote (with relict garnet) + quartz + calcite. Other silicates such as stilpnomelane, microcline, and a pale yellow biotite are locally observed, and a pale yellow tourmaline is found in some veinlets. Graphite is common (Lecouffe, 1987). Metallic associations include ubiquitous (commonly abundant) chalcopyrite and some sphalerite (locally with inclusions of stannite; Lecouffe, 1987) and arsenopyrite generally toward the marble. Pyrrhotite may contain inclusions of galena (in some cases rich in selenium and with inclusions of bismuth selenides; Lecouffe, 1987) and native bismuth, in some cases associated with bismuthinite, hessite, tetradymite, stannite, mackinawite, and native gold. Magnetite is rare and the relative chronology of its development is not known. Pyrite has been observed at a few places and generally appears to postdate pyrrhotite.

Amphibole compositions range from a ferroactinolite to a ferrous hornblende (Fig. 30). The ferrous hornblende is subordinate and appears only in direct contact with aluminous minerals (Fonteilles and Machairas, 1968). These amphiboles are sometimes Cl

rich (up to 0.24%) and their MnO content is in the range of 0.7 to 1.4 percent; epidote is in the range clinozoisite₅₀₋₆₀-pistacite₅₀₋₄₀.

In the granodiorite, the assemblage is pyrrhotite + scheelite + quartz + calcite + chlorite + albite \pm muscovite \pm biotite \pm pale yellow tourmaline \pm apatite \pm sphene. Tourmaline and apatite may be abundant in some veinlets. The metallic association is the same as in the hydrothermal rocks developed in the skarns.

In the skarns, scheelite of this stage is everywhere associated with pyrrhotite. The WO_3 content of the ore is highly variable from 0 to 40 percent. The average ore grade has been 1.4 percent in the Bois d'Anglade deposit and 1.9 percent in the Véronique deposit. The transition from barren to scheelite-bearing pyrrhotite may be either progressive or abrupt. The highest grade parts are in many cases in direct contact with the marble ("marble line"). Remnants of untransformed skarns, usually decimetric or less, commonly are observed within the pyrrhotite-scheelite ore.

In the granodiorite, scheelite occurs locally in small amounts (but locally with high grade) in altered areas, with or without pyrrhotite, but most of the scheelite found in the intrusive rocks occurs in silicified F_0 mylonites with quartz and some chlorite, usually without sulfides.

The average content of gold of ten samples of type 2 ore has been found to be 10 g/metric ton in the lower part of the Véronique Southeast orebody (elev 1110-1165 m). Previous assays on type 3 ore have given far lower grades of about 0.2 g/metric ton.

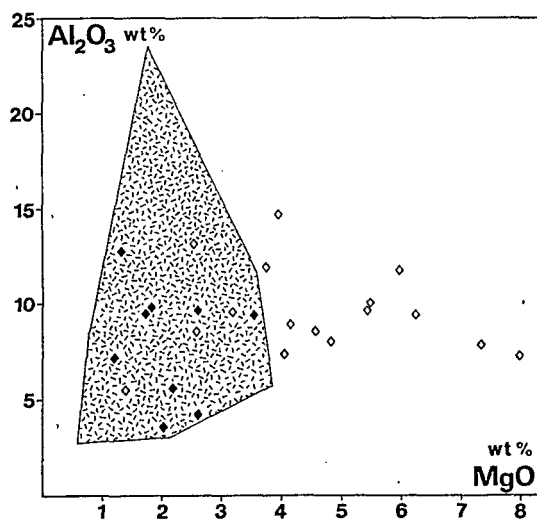


FIG. 28. MgO vs. Al_2O_3 for dark-colored calc-silicate hornfels skarns (black diamonds) and light-colored calc-silicate hornfels skarns (open diamonds). Stippled area is the envelope of compositions of the Barrégiennes plus calc-silicate hornfels. XRF analyses from Zahm (1987a).

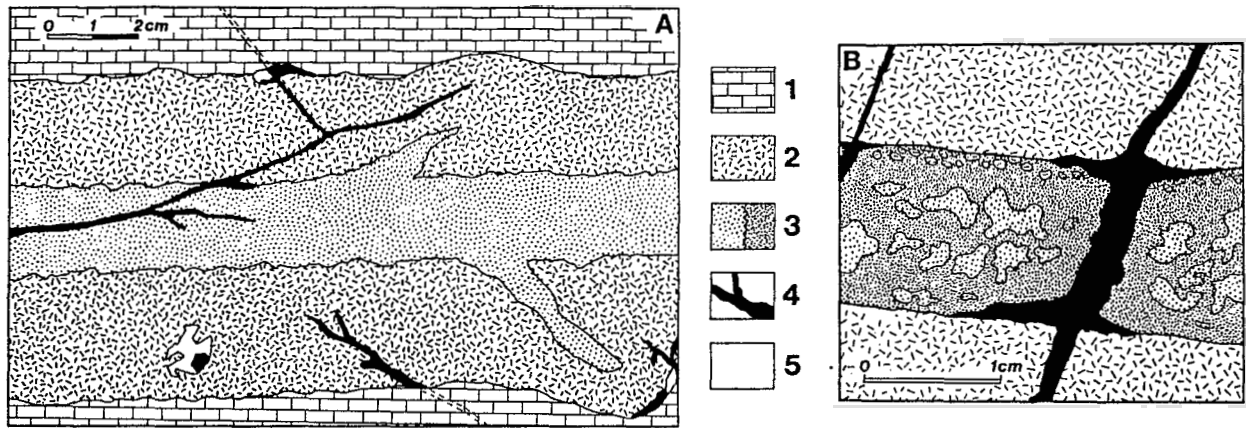


FIG. 29. A. An example of the distribution of late garnet in a zoned marble skarn. B. Relationship between early garnet and pyroxene, epidote (early hydrous calc-silicate), and late garnet in a calc-silicate hornfels skarn. 1 = marble, 2 = hedenbergite, 3 = primary garnet (light dots) and early epidote (heavy dots), 4 = late garnet, 5 = black quartz (modified from Fonteilles et al., 1988).

Pyrrhotite compositions have been determined by X-ray diffraction following the method of Toulmin and Barton (1964) and Arnold (1966) and by microprobe. Microprobe analysis by Soler (1977) (11 determinations) and Derré et al. (1984) (10 determinations) give values between 47.0 and 48.5 at. percent Fe. X-ray data (Soler, 1977; Krier-Schellen, 1988) show that pyrrhotite is the hexagonal polymorph. Twenty-one determinations on unmineralized and scheelite-bearing samples collected throughout the Bois d'Anglade deposit (Soler, 1977) and 11 from the Véronique deposit (Krier-Schellen, 1988) were performed (Fig. 31). Low-temperature superstructures have been observed in only four samples. The other samples give d_{102} between 2.0670 and 2.0727 Å, which corre-

sponds to 47.4 to 48.0 at. percent Fe in accordance with the equations of Toulmin and Barton (1964) or Yund and Hall (1969). No difference in composition appears between unmineralized and mineralized pyrrhotite. The pyrrhotite from the Véronique deposit, which belongs mainly to type 2 ore, appears to be slightly less Fe rich than the pyrrhotites from the Bois d'Anglade deposit which are mainly from type 3 ore.

The Fe content of sphalerite (microprobe determination, Derré et al., 1984) varies between 7.6 and 8.8 at. percent.

The As content of arsenopyrite (microprobe determination, Lecouffe, 1987; Fig. 32) varies from 35.7 to 33.3 at. percent. The fact that arsenopyrite from

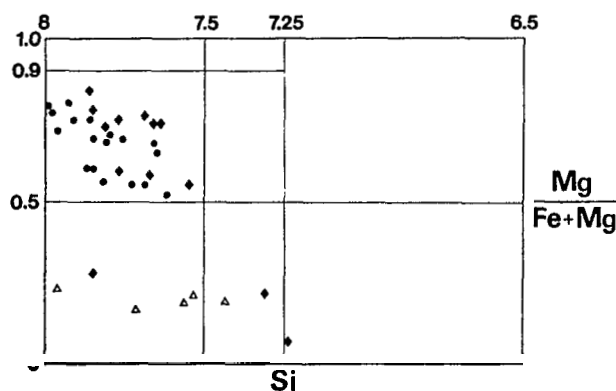


FIG. 30. Compositions of amphiboles (in calculated atom/unit formula; electron microprobe analyses from Zahm, 1987a). Symbols: open triangles = from the endoskarns, black diamonds = formed in the marble and calc-silicate hornfels skarns during late hydrothermal processes, black circles = formed on calc-silicate hornfels during the late hydrothermal processes.

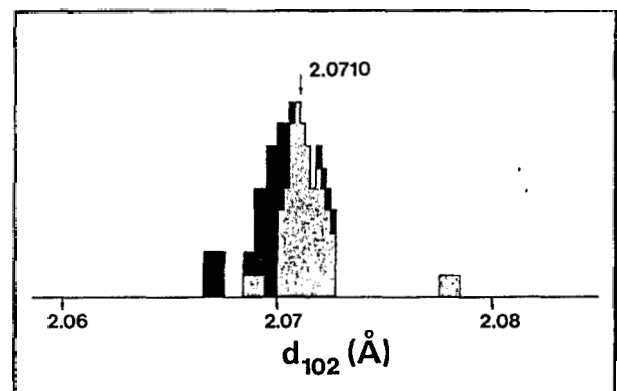


FIG. 31. d_{102} spacing (in Å) for pyrrhotites determined by X-ray diffraction. Dotted pattern = data from Soler (1977) for pyrrhotites from the Bois d'Anglade deposit (mainly type 3 ore), black = data from Krier-Schellen (1988) for pyrrhotites from the Véronique deposit (mainly type 2 ore).

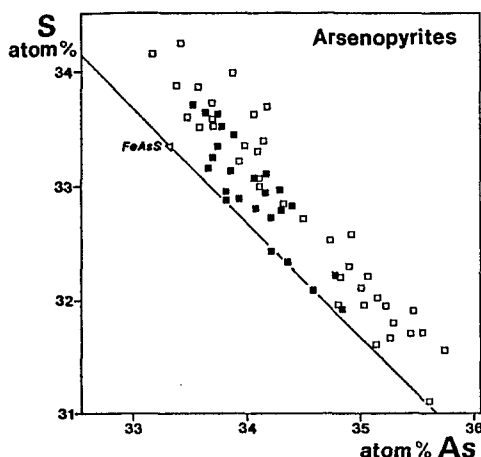


FIG. 32. As vs. S (at. %) for the arsenopyrite (electron microprobe analyses from Lecouffe, 1987). Black squares = in faults inside the granodiorite, open squares = in the orebodies outside the granodiorite.

the type 3 ore is richer in As may indicate the existence of gradients of f_{S_2} during ore deposition, as discussed below.

Andradite occurrence

Andradite has been found once in association with hedenbergite + pyrrhotite + pyrite + quartz + calcite in the Quer de l'Aigle showing (Zahm, 1987a). No petrographic or geologic evidence is available to ascertain the relations of this unique occurrence with the above stages. This rare association is restricted to vugs and/or blind veinlets, and as emphasized below, could be the result of a local evolution in a closed system.

Late veins

A series of mostly unmineralized late veins cut the orebodies and the adjacent terranes. Three types of veins may be distinguished: veins with quartz + coarse-grained pyrrhotite; geodic veins with sphalerite-chlorite-calcite and apophyllite, exceptionally mineralized in gold; and veins with prehnite and laumontite. Some of these veins contain well-crystallized isolated scheelite crystals. No alteration of host rocks is evident on the margins of those veins.

Estimation of P-T-X Conditions during Contact Metamorphism, Skarn Formation, and Late Alteration

The estimation of P-T-X conditions during the different stages of the evolution of the Salau deposit is based on the integration of the compositions of the silicate and sulfide minerals and experimental data, and/or thermodynamic calculations (Soler, 1977; Zahm, 1987a).

Contact metamorphism

Mineral assemblages in the inner metamorphic zone can be used to determine the P-T-X conditions during contact metamorphism. Both temperature and solid pressure may be regarded as constant within the inner zone, but gradients of fluid pressure and of fugacities (f_{CO_2} , f_{H_2O} , and f_{O_2}) may be expected since dehydration, decarbonation, and bleaching of carbonaceous matter are generally observed.

Regional geologic considerations lead to an estimation of the solid pressure at the top of the "granitoides en massifs supérieurs" in the Pyrenees of 2 kbars (Autran et al., 1970; Van Marcke de Lummen, 1983), and this is the value used in the calculations and with reference to the experimental data. It is probable that in this situation the fluid pressure (P_f) was lower than the solid pressure (P_s) during contact metamorphism (Autran et al., 1970). In some cases, the fluid pressure can be determined from the parageneses, since it is the only parameter to be considered in most hydrothermal experiments. Thermodynamic calculations permit the determination directly of f_{CO_2} but not X_{CO_2} , for which an estimation of P_f is needed. A further complication is due to the nonideal character of the H_2O-CO_2 mixtures (Ryzhenko and Malinin, 1971; Helgeson et al., 1978; Walther and Helgeson, 1980). In view of those difficulties, it is more reasonable to discuss the observed assemblages in a T- f_{CO_2} diagram rather than in a T- X_{CO_2} diagram.

In the zone of contact metamorphism where the skarns developed at a later stage, the main constraints on T- f_{CO_2} conditions are the presence of calcic aluminous garnet (grossular₈₃₋₉₄), epidote (pistacite₂₅₋₆₅), and calcic plagioclase and the rarity of wolastonite. Previous estimations (Soler, 1977) based on the experiments by Newton (1966), Gordon and Greenwood (1971), Holdaway (1972), Liou (1973), and Kerrick et al. (1973) and thermodynamic data (Robie and Waldbaum, 1968) have been updated using new experimental results (Kerrick, 1977; Taylor and Liou, 1978; Perchuk and Arenovich, 1979) and revised thermodynamic values (Robie et al., 1978; Robinson et al., 1983). Garnet solid solution has been considered as ideal, following Holdaway (1972) and Perchuk and Arenovich (1979); the model of solid solution proposed by Perchuk and Arenovich (1979) has been used for epidote.

The results are given in Figures 33 and 34. Considering $P_s = P_f = 2$ kbars, the estimated conditions of contact metamorphism in the innermost zone are $472^\circ C < T < 556^\circ C$ and $300 \text{ bars} < f_{CO_2} < 620 \text{ bars}$ ($0.05 < X_{CO_2} < 0.20$).

Graphite buffers of $\log f_{O_2}$ between -25.3 (for $T = 472^\circ C$ and $f_{CO_2} = 300 \text{ bars}$) and -22.2 (for $T = 556^\circ C$ and $f_{CO_2} = 620 \text{ bars}$) are present.

If we take into account that the fluid pressure is

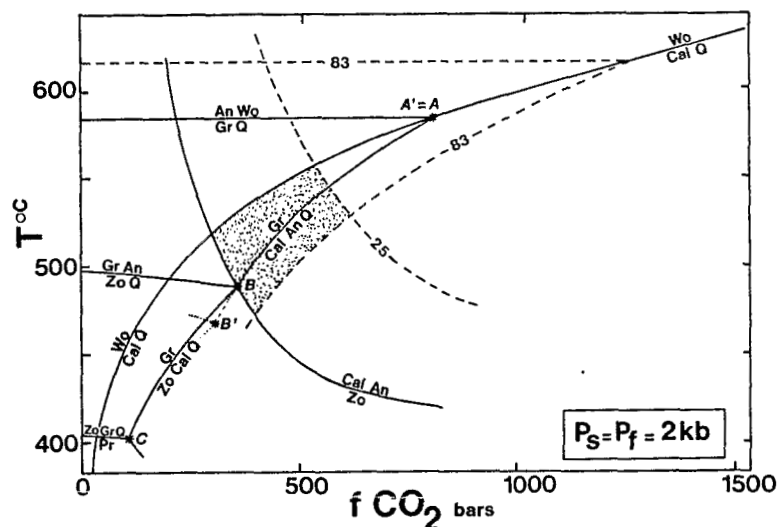


FIG. 33. f_{CO_2} vs. T ($^{\circ}\text{C}$) for the assemblages of the calc-silicate hornfels at $P_s = P_f = 2$ kbars (references in text). Dashed lines labeled 83 and 25 are the equilibria anorthite + wollastonite = grossular + quartz and grossular = calcite + anorthite + quartz for a garnet with 83 mole percent grossularite, and calcite + anorthite = zoisite for an epidote with 25 percent pistascite, respectively. A, B, and C = invariant points. In this representation, when considering $P_s = 2$ kbar and $P_f = 1$ kbar, point A is unchanged ($A' = A$), while B changes to B' .

lower than the solid pressure, for example, for a choice of $P_f = 1$ kbar or $P_s = 2$ kbars, the P - f_{CO_2} estimated conditions are not much different, but the calculated X_{CO_2} range is quite different ($0.15 < X_{\text{CO}_2} < 0.40$; Fig. 34).

Experimental data and thermodynamic calculations show that the presence of sphene (Hunt and Kerrick, 1977), salitic clinopyroxene (Slaughter et al., 1975), and vesuvianite (Ito and Arem, 1970; Hochella et al., 1982) does not produce any additional constraints. The absence of prehnite is consistent with the estimated conditions (Liou, 1971; Liou et al., 1983).

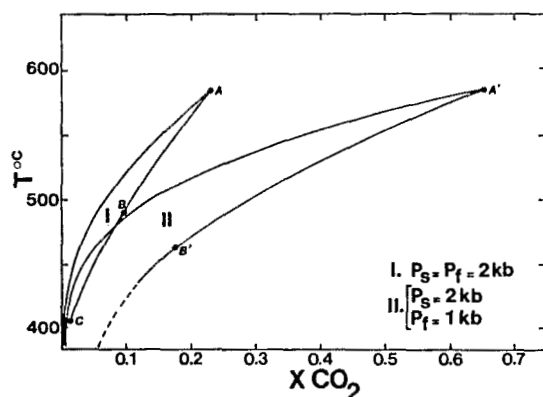


FIG. 34. Stability field of the assemblage grossular + calcite + quartz in the X_{CO_2} vs. T ($^{\circ}\text{C}$) diagram (modified from Soler, 1977). I = $P_f = P_s = 2$ kbars, II = $P_f = 1$ kbar, $P_s = 2$ kbars; A, B, C, A', and B' as in Figure 33.

Metasomatism

Primary skarns: In the case of Salau, estimation of the P-T-X conditions of formation of the primary skarns relies mainly on the existing data for the stability field of hedenbergite in the system Ca-Fe-Si-C-O. A detailed qualitative approach to this system has been given by Burt (1972; Fig. 35). On the basis of experimental data (Gustafson, 1974; Liou, 1974) and thermodynamic values (Robie and Waldbaum, 1968), Soler (1977) calculated the stability field of the association (pure) hedenbergite + calcite + quartz in the system Ca-Fe-Si-C-O. New experimental data (Gamble, 1982; Burton et al., 1982) and reconsidered thermodynamic values (Robie et al., 1978; Robinson et al., 1983) permit improvement of the previous estimates.

The development of a system of open veins at this stage of granite evolution in many granite apices shows that fluid pressure was in most cases higher than the lowest strain component. In such case, and for the present paper, the approximation $P_f = P_s$ may be reasonably retained. As a matter of fact, quartz and calcite are not primary minerals in the skarns. The conditions defined below are valid for a slightly later stage when quartz, calcite, and some pyrrhotite crystallize in the intergranular spaces, without any destabilization of hedenbergite. The estimation of the conditions of formation of hedenbergite alone must rely on an estimation of the chemical potential of iron, silica, and lime in the metasomatic fluids. Such a discussion has been undertaken by Soler (1977), who

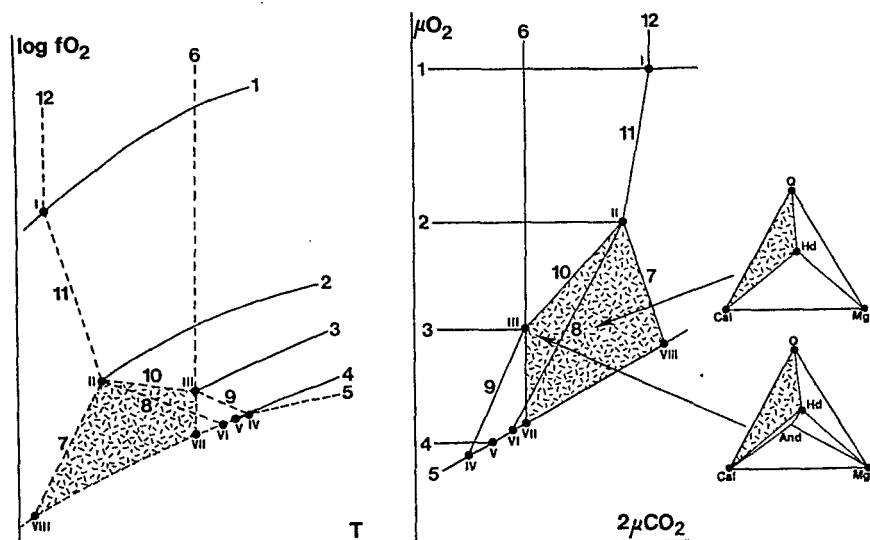


FIG. 35. Qualitative T - f_{O_2} and μ_{O_2} - $2\mu_{CO_2}$ diagrams illustrating the stability fields of minerals in the system Ca-Fe-Si-C-O (modified from Burt, 1972). The stippled area corresponds to the stability of the association hedenbergite + calcite + quartz. Reactions as follows: 1, magnetite + O_2 = hematite; 2, hedenbergite + O_2 = andradite + magnetite + quartz; 3, hedenbergite + wollastonite + O_2 = andradite + quartz; 4, magnetite + quartz = fayalite + O_2 ; 5, C + O_2 = CO_2 ; 6, quartz + calcite = wollastonite + O_2 ; 7, hedenbergite + CO_2 + O_2 = magnetite + calcite + quartz; 8, hedenbergite + magnetite + calcite + O_2 = andradite + CO_2 ; 9, hedenbergite + calcite + O_2 = andradite + wollastonite + CO_2 ; 10, hedenbergite + calcite + O_2 = andradite + quartz + CO_2 ; 11, andradite + CO_2 = magnetite + calcite + quartz + O_2 ; 12, andradite + CO_2 = hematite + calcite + quartz. Dots with roman numerals characterize the invariant points.

showed that the stability of hedenbergite implies that the fluid was nearly saturated with respect to magnetite and quartz during primary skarn formation (see also Brown et al., 1985).

Results concerning the stability of the association hedenbergite + calcite + quartz are synthesized in Figures 36 and 37. A detailed discussion of this diagram is given by Soler (1977) and Fonteilles et al. (1980). Assuming that the highest possible temperature obtained for the contact metamorphism in the innermost zone (556°C, Fig. 33) is also the highest possible temperature at the metasomatic stage, and assuming that $P_f = P_s = 2$ kbars, the following conditions have been estimated (Fig. 36): 340°C < T < 556°C, $-31.4 < \log f_{O_2} < -19.9$, and $f_{CO_2} > 70$ bars.

As shown by fluid inclusion studies (see below), the fluids at this stage were CO_2 poor. At a given f_{CO_2} , conditions are much more restricted as emphasized in Figure 37.

Moreover, when considering the presence of water, the stability field of hedenbergite is limited at low temperatures by the reaction hedenbergite + CO_2 + O_2 = Fe actinolite + calcite + quartz (equilibrium 13). On the basis of the experimental results of Ernst (1966) on the equilibrium Fe actinolite = hedenbergite + fayalite + quartz + H_2O , thermodynamic values for ferroactinolite and the conditions of equilibrium

(13) have been calculated. For $P_s = P_f = 2$ kbars, the reaction occurs at 440°C ($f_{CO_2} = 1,000$ bars), 407°C ($f_{CO_2} = 500$ bars), or 350°C ($f_{CO_2} = 100$ bars; Figs. 36 and 37).

The presence of pyrrhotite in association with hedenbergite, calcite, and quartz at this stage brings additional constraints on the possible P-T-X conditions (Fig. 38). The composition of pyrrhotite at this stage is nearly constant at $Fe_{0.914}S$ and defines a T - $\log f_{S_2}$ relation (e.g., Barton and Skinner, 1979). On the basis of the thermodynamic values for pyrrhotite $Fe_{0.914}S$ (see Soler, 1977, for calculations), P-T-X conditions for equilibrium (14), hedenbergite + S_2 = pyrrhotite + calcite + quartz + O_2 , may be calculated. For f_{CO_2} in the range 500 to 1,000 bars, conditions for equilibrium (14) are almost the same as for the C + O_2 = CO_2 buffer (equilibrium 5).

When entering the calcic rocks, the metasomatic fluid was nearly saturated with respect to quartz and transported iron, manganese, and aluminum. No evidence of magnesium addition is available.

In the marble skarns, hedenbergite has a very low Mg content and virtually no acmite component in solid solution and magnetite is characteristically absent. Therefore Mg/Mg + Fe in the fluid was much lower than Mg/Mg + Fe in the hedenbergite in view of the exchange isotherms experimentally determined by Uchida and Iiyama (1980) and Iiyama (1984). Then

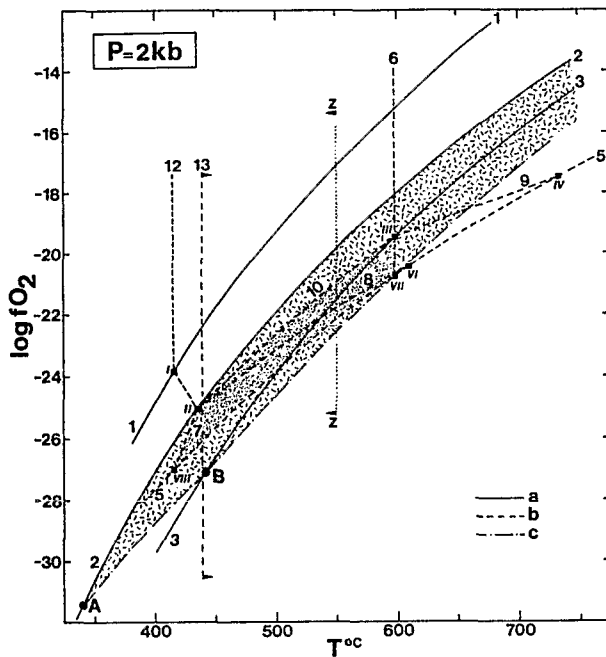


FIG. 36. $\log f_{O_2}$ - T ($^{\circ}C$) diagram illustrating the stability field of minerals in the system Ca-Fe-Si-C-O with $P = 2$ kbars (modified from Soler, 1977). Reaction numbers as in Figure 35. Reaction (4) has been omitted for clarity. Reaction (13) is hedenbergite + CO_2 + H_2O = ferro-actinolite + calcite + quartz (discussion in text). a = f_{CO_2} independent curves, b = f_{CO_2} dependent curves, drawn for $f_{CO_2} = 1,000$ bars, c = lower limit of the stability field of hedenbergite + calcite + quartz (see Soler, 1977, for a detailed discussion). Point A corresponds to the invariant assemblage quartz + calcite + hedenbergite + andradite + graphite + magnetite. Point B corresponds to the invariant assemblage quartz + calcite + hedenbergite + andradite + graphite + wollastonite. The stippled area is the stability field of hedenbergite + calcite + quartz. The dotted area is the stability field of hedenbergite + calcite + quartz with $f_{CO_2} = 1,000$ bars. ZZ is the upper temperature limit indicated by the study of contact metamorphism. Dots with roman numerals characterize the invariant points.

the enrichment in MgO in the light-colored calc-silicate hornfels skarns corresponds to a downstream displacement of MgO from the dark-colored skarns according to a model by Guy (1988).

Early hydration of skarn minerals and late-stage garnet: The reactions corresponding to the formation of epidote at the expense of the primary garnet and of amphibole (ferro-actinolite) at the expense of the hedenbergitic pyroxene have been discussed in the previous sections. As no drastic release of the solid pressure nor drastic increase of the fluid pressure may be supposed at this stage, factors favoring both reactions would be a decrease of temperature and/or an increase of the fugacity of carbon dioxide. Maximum temperature, corresponding to the reaction $garnet_{33} + fluid = epidote_{33} + calcite + quartz$, is slightly lower than $500^{\circ}C$. Assuming a continuous decrease of the temperature of the fluids, the mini-

imum temperature defined for the later hydrothermal stage ($\approx 400^{\circ}C$, see below) would be valid for the present stage. Then late hydration of primary skarn minerals would have occurred between 400° and $500^{\circ}C$. This interval is almost the same as the interval proposed for the formation of the primary skarn. Thus, the hydration of primary skarn minerals would mainly be the result of an increase in f_{CO_2} in the late stage of skarn formation. Epidotization of garnet is very common and amphibolitization of pyroxene is limited at this stage, which implies a limited increase of f_{CO_2} . This limited increase and the following decrease which leads to the formation of late-stage garnet would correspond to fluctuations in time and perhaps in space of the compositions of the fluids. Since isotopic data (see below) suggest that early-stage CO_2 carbon is of magmatic origin, such fluctuations might correspond to an irregular degree of mixing with a fluid originating in the country rock.

Late hydrothermal processes

Characterization of the P-T-X conditions for the late hydrothermal processes is based on the assemblages of sulfide and silicate minerals.

Reliable estimation of the P-T- f_{S_2} conditions may be deduced from the compositions of pyrrhotite (e.g., Barton and Skinner, 1979) and arsenopyrite (e.g., Kretschmar and Scott, 1976; Sharp et al., 1985) and the systematic presence of native bismuth and in some cases bismuthinite. The T- $\log f_{S_2}$ diagram of Figure 39 illustrates the rather large domain where pyrrhotite and arsenopyrite of the observed compositions and bismuth are stable. The lowest possible tem-

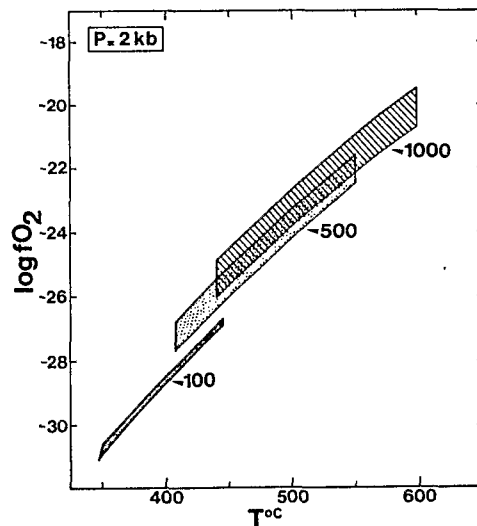


FIG. 37. $\log f_{O_2}$ - T diagram illustrating the stability field of the assemblage hedenbergite + calcite + quartz at $P = 2$ kbars, with $f_{CO_2} = 1,000, 500,$ and 100 bars, respectively.

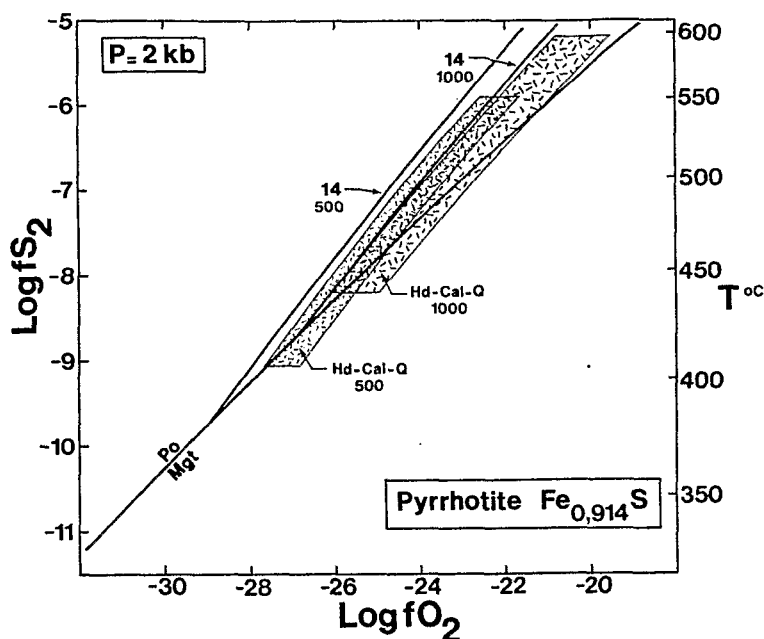


FIG. 38. $\log f_{O_2} - \log f_{S_2}$ (or $T^\circ C$) diagram illustrating the relative position of the stability field of the assemblage hedenbergite + calcite + quartz and of the equilibrium (14) hedenbergite + CO_2 + S_2 = pyrrhotite + calcite + quartz + O_2 , for $f_{CO_2} = 1,000$ and 500 bars, respectively. Calculations have been made using the mean composition $Fe_{0.914}S$ for pyrrhotite.

perature for this assemblage is nearly $400^\circ C$ with $\log f_{S_2} \approx -10$. Assuming a continuous decrease in the temperature of the fluids, the maximum temperature determined for the previous stage (hydration of the primary skarn minerals) would also be valid for the hydrothermal stage; then $T \leq 500^\circ C$ and $\log f_{S_2} \leq -6$ at this stage. The spectrum of composition of the arsenopyrite and the pyrrhotite suggests f_{S_2} gradients during this stage. In particular, pyrrhotite is more Fe rich and arsenopyrite more As rich in type 3 ore than in type 2 ore. As type 3 ore appears to be a distal extension of type 2 mineralization, this evolution of the compositions of pyrrhotite and arsenopyrite at the mine scale would be linked with decreasing f_{S_2} (mainly) and temperature downstream.

At a later stage, arsenopyrite is not present and the assemblage is pyrrhotite + bismuth + bismuthinite; at this stage the pyrrhotite has the same range of composition (47.4–48.0% Fe), which implies a continuity in the $f_{O_2} - f_{S_2}$ buffering process of the fluid in the source region but which does not place additional constraints on the temperature of ore formation at this stage. Fluid inclusion studies (see below) suggest a minimum temperature of $\approx 350^\circ C$. The absence of magnetite yields an upper limit for f_{O_2} at each temperature, through the equilibrium pyrrhotite + O_2 = magnetite + S_2 (Fig. 38), and the presence of graphite in the ore gives a minimum for f_{CO_2} for a given temperature. A mean estimate at this stage

would be $T = 425^\circ C$, $-9 < \log f_{S_2} < -7.5$, $\log f_{O_2} < -27.0$, and $f_{CO_2} < 1,000$ bars (where graphite is present).

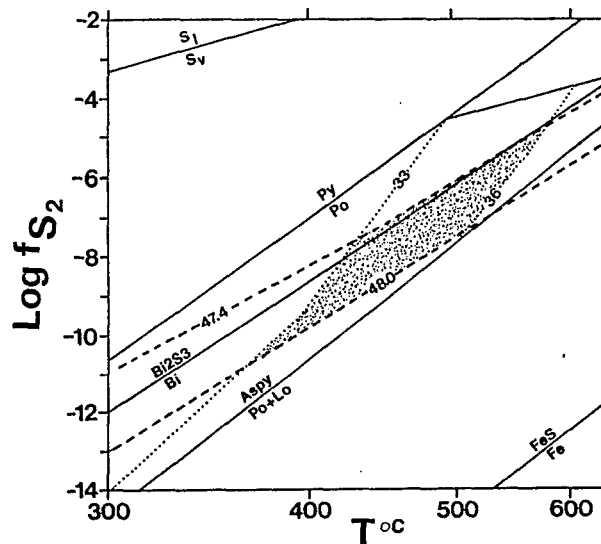


FIG. 39. f_{S_2} vs. T ($^\circ C$) diagram for the hydrothermal sulfide assemblage pyrrhotite + arsenopyrite. Stippled pattern shows limits of assemblage. Fe content of pyrrhotite (following Barton and Skinner, 1979) shown by dashed lines. As content of arsenopyrite (following Kretschmar and Scott, 1976) shown by dotted lines.

The rare hedenbergite + pyrite + pyrrhotite + quartz + calcite \pm andradite assemblage observed by Zahm (1987a) in the Quer de l'Aigle showing allows an independent estimation of T , f_{S_2} , and f_{O_2} . The pyroxene from the assemblage with andradite is hedenbergite_{93.94} diopside_{1.3} johannsenite_{4.6}, whereas in the assemblage without andradite, the pyroxene is hedenbergite₈₅ diopside₁₀ johannsenite₅. Both are at equilibrium with pyrite and pyrrhotite, according to Zahm (1987a). Assuming a pressure of 2 kbars and combining the experimental results of Burton et al. (1982) and Gamble (1982) dealing with the influence of the johannsenite and diopside content of hedenbergite, respectively, on the equilibrium hedenbergite + S_2 = andradite + pyrite + quartz and experimental data on the equilibrium pyrite-pyrrhotite (Toulmin and Barton, 1964; Barton and Skinner, 1979; Fig. 40) the following conditions are estimated: $330^\circ\text{C} < T < 370^\circ\text{C}$, $-9.7 < \log f_{S_2} < -8$. $\log f_{O_2}$ may be determined on the basis of the experimental data by Gustafson (1974), Burton et al. (1982), and Gamble (1982). At $T = 350^\circ\text{C}$, Zahm (1987a) obtained $-33.1 < \log f_{O_2} < -29.6$. Both experimental data on the reaction andradite + CO_2 = quartz + calcite + FeO_x (Taylor and Liou, 1978) and our previous calculations dealing with the association hedenbergite + calcite + quartz imply a very low f_{CO_2} (70 bars $< f_{\text{CO}_2} < 100$ bars - $X_{\text{CO}_2} < 0.05$) at this stage.

With respect to T - f_{S_2} conditions, the results are in apparent contradiction with those deduced from the main silicate-sulfide assemblage (Fig. 40). The uniqueness of this association, namely, the elevated number of minerals, suggests that it did not crystallize in an open system, where the activities and chemical potentials are partly imposed by the fluid and the number of phases is lowered (e.g., Korzhinskii, 1969; Fonteilles, 1979). This association appears to be the end product of a local evolution in a closed system (i.e., in a blind veinlet or vug) and the estimated conditions have only a local meaning. The same explanation would be valid for the sporadic presence of pyrite.

Note that the conditions deduced for this particular association are consistent with the Holland (1965)'s isochemical evolution ("main line"), whereas the general evolution at Salau corresponds to a clearly lower f_{S_2} which appears to be buffered by some medium external to the deposit itself.

Fluid Inclusion Studies

Two hundred samples were selected for microthermometric analysis and 11 for Raman spectrometry (Krier-Schellen, 1988). The host minerals of fluid inclusions in the skarns are grossularite, hedenbergite, scheelite, and quartz. No fluid inclusions were studied in the late garnet. Early hydrothermal minerals containing analyzed fluid inclusions are quartz and

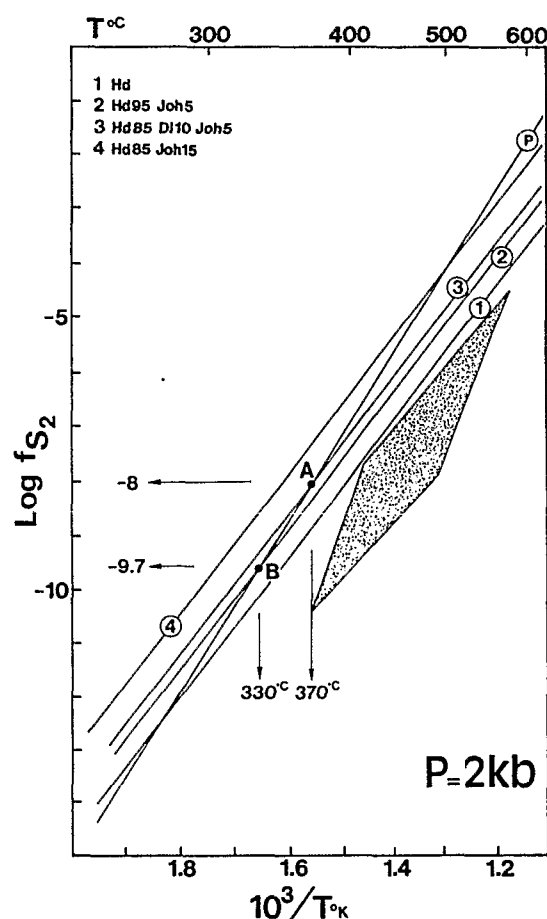


FIG. 40. Equilibrium hedenbergite = andradite + pyrrhotite (or pyrite) + quartz in air f_{S_2} vs. T ($^\circ\text{C}$) diagram considering various composition of the pyroxene (1 to 4), following Burton et al. (1982) and Gamble (1982). P = equilibrium pyrite = pyrrhotite (Barton and Skinner, 1979). The observed assemblages andradite + hedenbergite + pyrite + pyrrhotite and hedenbergite + pyrite + pyrrhotite (from Zahm, 1987a, comments in text) are stable along P between A and B. The stippled area corresponds to the conditions defined in Figure 39. Di = diopside, Hd = hedenbergite, Joh = johannsenite.

scheelite. Finally, fluid inclusions in calcite from the late veins were investigated. Some measurements were also performed on quartz grains in the granodiorite. Measurements were performed on 10- to 20- μm inclusions.

Types of fluid inclusions

Three types of fluid inclusions have been identified: type I: high-salinity aqueous inclusions, containing about 5 vol percent vapor and in some cases halite crystals; type II: carbonic aqueous inclusions, with variable degrees of filling; and type III: hybrid inclusions presenting features of both former types of inclusions.

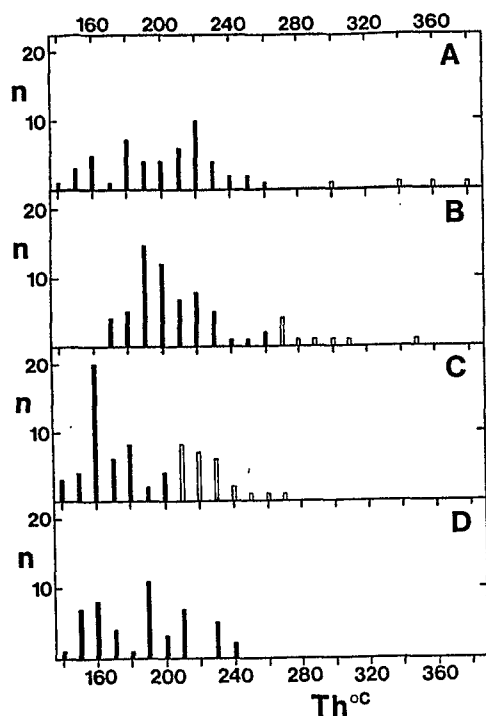


FIG. 41. Homogenization temperatures of fluid inclusions (from Krier-Schellen, 1988). Open bars = primary inclusions, black bars = secondary inclusions, A = granodiorite, B = primary skarns, C = pyrrhotite + scheelite + quartz ore, D = late hydrothermal veins.

Type I fluid inclusions are found in all the minerals listed above. Types II and III are only found in quartz and scheelite associated with pyrrhotite in the hydrothermal stage. The three types of fluid inclusions may occur in the same host mineral.

There is a definite distribution of the various types of fluid inclusions. Type I inclusions are found in all parts of the deposit. Type II occur only in the lowest

visible part of the deposit, especially at the 1230 level of Véronique (Fig. 14). Type III have only been found at intermediate levels, between about 1320 and 1446.

Microthermometric results

Type I: Final melting temperatures and halite dissolution temperatures of type I fluid inclusions give salinities in the range of 23 to 30 equiv wt percent NaCl. This salinity bracket is remarkably constant throughout the deposit as well as during all the metasomatic and hydrothermal stages. As noted previously for f_{s_2} , the salinity at the source of the fluid must then have been buffered by some medium external to the deposit itself, and may be indicative of the source region. The distribution of homogenization temperatures shows a series of peaks (Fig. 41) indicating several influxes of the same fluid with decreasing temperature. These influxes probably were controlled by successive opening of faults.

Several isochores have been determined following data in Potter and Brown (1977) (Fig. 42). Brackets of trapping temperatures may then be estimated for the successive batches of type I fluid, using as a minimum pressure the geologic estimate (2 kbars), and as a maximum pressure, the upper pressure estimated by $f_{s_2} - T$ geothermobarometry (see below). Several temperature intervals representing the main batches for the primary fluid inclusions of the initial skarn stage are bracketed between 455° and 570°C, in very good agreement with the thermodynamic estimation presented in the previous section. The other intervals show the successive hydrothermal stages and also appear to be in accordance with the temperatures estimated previously.

Type II: The final melting temperature of a solid phase in type II fluid inclusions lies between -80° and -57°C. Final melting of clathrate lies between 7° and 20°C, indicating variable amounts of CO₂ and

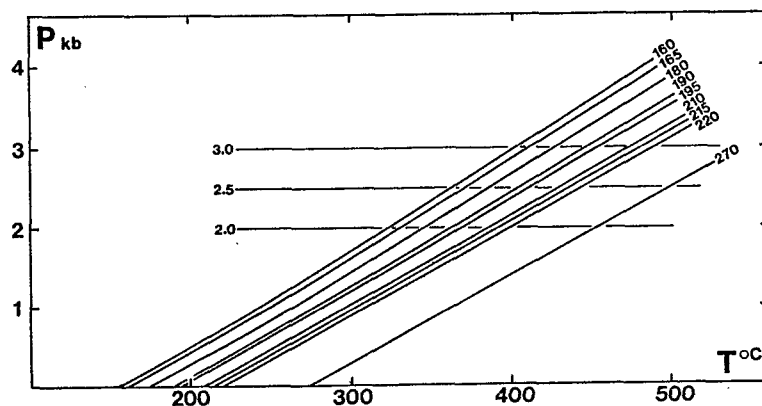


FIG. 42. Isochores for the H₂O-NaCl type I fluid inclusions. Isochores are labeled by their homogenization temperature (data from Krier-Schellen, 1988).

TABLE 4. Temperatures (°C) of Trapping of Type I (saline hydrous) Fluid Inclusions

Granodiorite	Primary skarns	Pyrrhotite ore	Hydrothermal veins
	455-540		
397-485	397-485	382-470	390-498
343-425	360-455	343-425	367-450
320-400		320-400	327-410

Data from Krier-Schellen (1988)

CH₄. Partial homogenization occurs in the liquid phase, indicating high-density inclusions. Total homogenization occurs between 280° and 360°C.

Type III: Some of the carbonic inclusions contain also a halite crystal and some of the high-salinity inclusions exhibit a final melting temperature corresponding to the clathrate melting.

Raman microprobe results

Nine type II fluid inclusions were analyzed by Raman spectrometry (CREGU, Nancy, France) in quartz samples of the type 2 ore from the F₁ fault in the 1230 level of the Véronique deposit: samples 20/2, 25/3, 25/5, and 25/27 were collected at the borders of the orebody, whereas samples 24/7, 24/10, 24/19, 24/24, and 28/4 were collected in the center of the orebody.

The results are given in Table 5. H₂O values were obtained by visual estimation of the volume ratio of the aqueous phase. Densities were obtained by combining Raman data with microthermometry data, following Swanenberg (1979) and Herskowitz and Kisch (1984) algorithms. Samples 24/7, 24/19, and 25/7 could not be correctly interpreted. For the six remaining inclusions, a modified Redlich-Kwong equation of state (Jacobs and Kerrick, 1981; Kerrick and Jacobs, 1981) has been used to calculate isochores in the P-T plane (Fig. 43). For each inclusion two isochores have been plotted taking into account the uncertainty on the visual estimation of the aqueous fill-

ing. Ignoring fluid inclusion 25/3, which probably underwent natural decrepitation, two groups of fluid inclusions may be distinguished: a high-pressure one represented by samples 20/2 and 25/5 and a moderate-pressure one represented by samples 24/10, 24/24, and 28/4. The latter group, which better fits geologic observations, is retained as representing the main fluid pressure. The former may be interpreted as local or rather early fluid overpressure preserved near or at the border of the skarn lenses.

T-f_{S₂} geothermobarometry

A new geothermobarometer based on the association of pyrrhotite and an H₂S-bearing fluid has been proposed by Krier-Schellen (1988). The intersection of the pyrrhotite solid solution isopleths and the type II fluid isopleths, based on the Raman microprobe data, provides an estimate of the temperature, whereas the pressure is linked with the temperature by the isochores of the fluid. The results are varied, depending upon the referred pyrrhotite solid solution isopleths (Fig. 44). Using the Rau's (1976) data, the following conditions were obtained by Krier-Schellen (1988): 335°C < T < 363°C, -9.51 < log f_{S₂} < -8.45, 2.160 < P(bars) < 2.580, and the reaction CH₄ + 2O₂ = 2H₂O + CO₂ in the fluid provides also an estimation for f_{O₂} (-32.8 < log f_{O₂} < -30.2). Krier-Schellen emphasized that these results are consistent with those determined by Zahm (1987a, see above) for the assemblage with andradite. However, it seems better to use the pyrrhotite solid solution isopleths from Barton and Skinner (1979) (Fig. 44) because (1) they are at present the standard reference data, (2) using Rau's data for the Salau pyrrhotite leads to the conclusion that pyrite should occur massively in the ore at equilibrium with pyrrhotite, which is definitely not the case, and (3) they provide estimates which are in agreement with the normal open-system conditions for pyrrhotite deposition: 405°C < T < 446°C, -8.6 < log f_{S₂} < -7.5, 2.500 < P(bars) < 3,000. The Froese and Gunter (1976) data on pyrrhotite isopleths provide estimates which are midway between the two former estimates.

TABLE 5. Raman Spectrometry Data for Selected Type II (H₂O, CO₂, CH₄) Fluid Inclusions

Sample and sample no.	H ₂ O	CO ₂	CH ₄	N ₂	H ₂ S	Density
1. 24/24	67.09 ± 4.36	5.80 ± 0.47	25.74 ± 3.69	1.23 ± 0.18	0.158 ± 0.028	0.60 ± 0.03
2. 20/2	80.88 ± 2.63	6.39 ± 0.64	10.25 ± 1.91	0.42 ± 0.08	0.063 ± 0.013	0.81 ± 0.02
3. 25/3	16.1 ± 16.1	64.3 ± 12.2	9.90 ± 1.97	9.72 ± 1.93	0.0000	0.66 ± 0.02
4. 24/10	56.22 ± 5.58	29.1 ± 3.53	11.38 ± 1.59	3.23 ± 0.45	0.079 ± 0.011	0.72 ± 0.02
5. 25/5	52.55 ± 5.75	39.77 ± 4.76	4.39 ± 0.57	3.3 ± 0.42	0.0000	0.87 ± 0.01
6. 28/4	55.27 ± 5.68	39.7 ± 5.0	2.87 ± 0.39	2.1 ± 0.29	0.094 ± 0.013	0.82 ± 0.01

Data, in mole percent, from Krier-Schellen (1988); in Figure 43, inclusions are referred to as 1 to 6 only

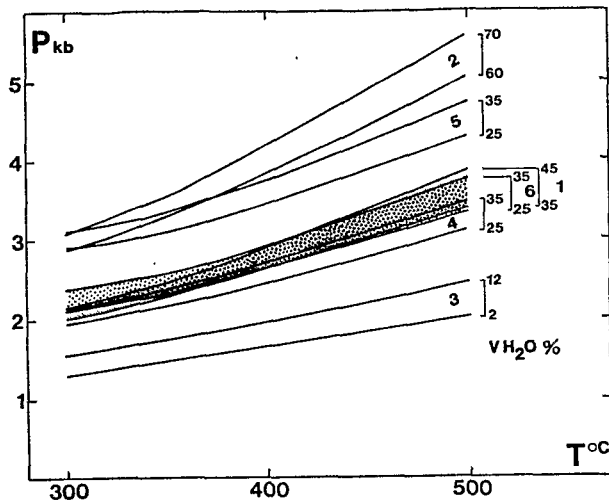


FIG. 43. Isochores in the P-T plane for six $\text{H}_2\text{O}-\text{CO}_2-\text{CH}_4$ (type II) inclusions (numbers 1 to 6 refer to the studied inclusions of Table 5). $V_{\text{H}_2\text{O}}$ is the volume ratio occupied by H_2O . To take into account the uncertainty upon the visual estimation of $V_{\text{H}_2\text{O}}$, for each inclusion isochores have been drawn for two values of $V_{\text{H}_2\text{O}}$ (from Krier-Schellen, 1988).

Interpretation

The first recorded fluid in the La Fourque granodiorite and surrounding rocks appears to be an $\text{H}_2\text{O}-\text{NaCl}$ type I fluid at a temperature of about 500°C . This fluid was responsible for the formation of the primary skarns. It had a relatively high salinity (about 25 wt %) and a relatively low oxygen fugacity ($\log f_{\text{O}_2}$ about -23). The salinity was buffered by an external medium, possibly in equilibrium with magmatic rocks at depth. The channelways of these fluids were mainly controlled by F_1 faults. Small amounts of scheelite and pyrrhotite were deposited at that time.

The fluids evolved thereafter continuously with decreasing temperature and f_{O_2} , with the salinity remaining constant. Hydration or dissolution of the early silicates and massive precipitation of pyrrhotite and scheelite formed the economic ore in several steps.

An $\text{H}_2\text{O}-\text{CO}_2-\text{CH}_4$ type II fluid then invaded some parts of the deposit. This fluid is characterized by a highly variable composition, a low f_{O_2} (between QFM and graphite buffers), a relatively low f_{S_2} (under the pyrite-pyrrhotite equilibrium) and a temperature which may be 350° to 450°C depending on the experimental data used. The rather natural idea that massive precipitation of scheelite has occurred particularly as a result of mixing between both types of fluids is not supported by the fact that the ore is as rich and of the same type in the upper part of the mine (where no type II fluid has been found) as in the lower part.

Stable Isotope Study

Stable isotope studies were undertaken by Guy (1979, 1980) and Toulhoat (1982). Detailed analytical procedures and results are given in their publications. These data have been recently synthesized and discussed by Guy et al. (1988).

C and O isotope compositions of carbonates

The $^{18}\text{C}/^{12}\text{C}$ and $^{18}\text{O}/^{16}\text{O}$ ratios of carbonates from the Salau deposit are plotted in Figure 45 (data from Guy, 1979, 1980), with reference to the limestone box ("LMS" represents the isotopic composition of most diagenetically altered limestones; e.g., Keith and Weber, 1964) and the primary magmatic carbon box ("PMC" includes the isotopic compositions of most primary magmatic carbonates; e.g., Taylor et al., 1967; Sheppard and Dawson, 1975; Deines, 1980).

Carbonates from the country rock (Salau Formation) have C isotope compositions indistinguishable from the limestone values but show O isotope compositions which may be similar to these values or depleted in ^{18}O . The most ^{18}O -depleted samples come from the contact zone with skarns.

Carbonates corresponding to the metasomatic and hydrothermal stages are indistinguishable one from the other. Both are strongly depleted in ^{13}C relative to the limestone values and show O isotope values

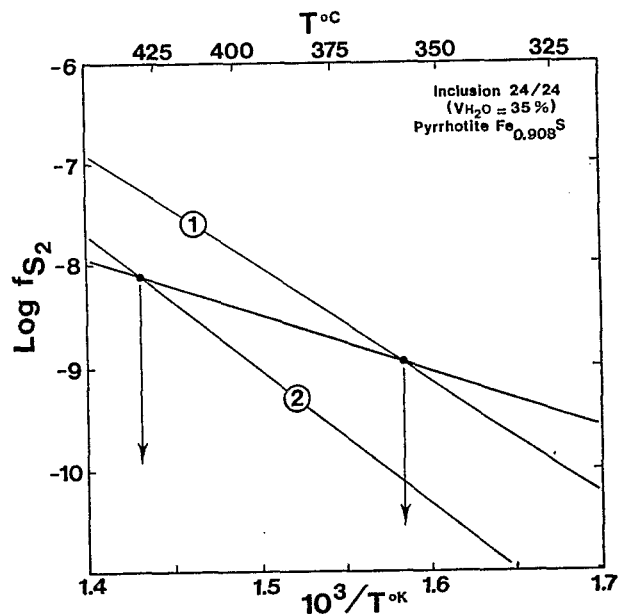


FIG. 44. $\log f_{\text{S}_2} - 1,000/T$ ($^\circ\text{K}$) diagram for the fluid inclusion 1 of Figure 43 with $V_{\text{H}_2\text{O}} = 35$ percent. The intersection of the isopleth of inclusion 24/24 (1 in Fig. 43) and the f_{S_2} -T relation corresponding to the coexisting pyrrhotite ($\text{Fe}_{0.908}\text{S}$) (lines labeled 1 and 2) defines the f_{S_2} -T conditions of deposition. Two possible f_{S_2} -T relations have been considered for the pyrrhotite: 1 = following Rau (1976), 2 = following Barton and Skinner (1979).

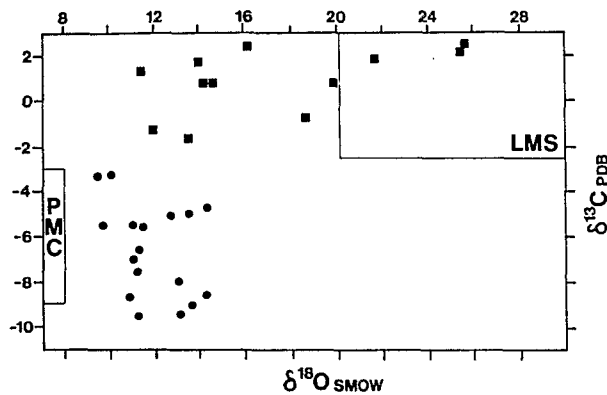


FIG. 45. $\delta^{18}\text{O}_{\text{SMOW}}$ vs. $\delta^{13}\text{C}_{\text{PDB}}$ diagram for calcite (data from Guy, 1979 and Guy et al., 1988). Black squares = calcite from country rock, black circles = calcite of metamorphic or late hydrothermal stages, PMC = primary magmatic carbon box, LMS = diagenetically altered limestones box.

similar to the more depleted samples of the country rock or even slightly more depleted.

These results are very similar with those obtained by most workers in the field of skarn-type deposits (e.g., Taylor and O'Neill, 1977). As discussed in some detail by Guy et al. (1988), two fundamentally different interpretations are possible for the hyperbolic shaped field of Figure 45.

A *magmatic-hydrothermal model* would have the compositions of the carbonates represented by various mixtures between the initial limestones values and magmatic carbon and oxygen. CO_2 carbonate, C isotope fractionation factors are essentially independent of temperature for $T > 300^\circ\text{C}$, so that the large range in $\delta^{13}\text{C}$ values reflects simply the large range of magmatic C to limestone C ratios. Since the C/O atomic ratios of the two poles are unlikely to be the same, such a mixing model will not, in general, generate calcites whose isotopic compositions plot on a straight line between the primary magmatic carbonates and the altered limestones. This model has been advocated by most workers in the field of skarns (e.g., Taylor and O'Neill, 1977; Guy, 1979, 1980; Bowman et al., 1985a and b; Brown et al., 1985; Valley, 1986).

An alternative hydrothermal-decarbonation model is proposed by Guy et al. (1988). The $\delta^{13}\text{C}$ values of calcites of the metamorphic and hydrothermal stages are interpreted in terms of a Rayleigh distillation or continuous CO_2 fluid removal process from limestone carbonates; the $\delta^{18}\text{O}$ values are viewed as the result of a hydrothermal exchange process with an externally derived fluid. Carbon and oxygen would not therefore be coupled because the mass of O in the CO_2 is relatively minor compared with the quantity of H_2O oxygen as shown by the relatively low X_{CO_2} in the fluids. The strict limitation of $\delta^{13}\text{C}$ at -10 per mil compared with other (unmineralized) skarns in the Pyrenees for

which $\delta^{13}\text{C}$ may be as low as -16 per mil is unexplained in this second model.

O and H isotope compositions of silicates

A few D/H and $^{18}\text{O}/^{16}\text{O}$ measurements have been performed by Toulhoat (1982) on OH-bearing silicates from the la Fourque granodiorite (biotite, chlorite, muscovite of the greisen stage) and from syn- and postmineralization hydrothermal veins (biotite, chlorite, amphibole). The data are synthesized in Figure 46.

The H and O isotope compositions of water in equilibrium with these minerals have been calculated for $T = 300^\circ\text{C}$ using the fractionation factors given by Taylor (1974), Susuoki and Epstein (1976), Friedman and O'Neill (1977), and Graham et al. (1984, 1987). The calculated isotopic composition of water will not change significantly if the assumed temperature is varied from 250° to 400°C .

Two groups of D/H values have been determined for the fluid.

A first group has $\delta\text{D} \approx -50$ per mil. The corresponding fluid could be of magmatic or metamorphic origin. It is of some interest to note that the analyzed amphibole (Fig. 46), although late with respect to the main hydrothermal stage, was in equilibrium with such a fluid.

A second group has $\delta\text{D} \approx -10$ per mil. This fluid could be of meteoric, sea, formation, or metamorphic origin (e.g., Sheppard, 1986). Toulhoat (1982) and Guy et al. (1988) favor a meteoric origin for this fluid. The $\delta^{18}\text{O}$ values are consistent with this interpretation but imply that the $\delta^{18}\text{O}$ of the fluid was partly controlled by the host rock (i.e., the water/rock ratio was low to moderate).

These results are in good agreement with petrological and fluid inclusion studies. The second "heavy" fluid would correspond to the $\text{H}_2\text{O}-\text{CO}_2-\text{CH}_4$

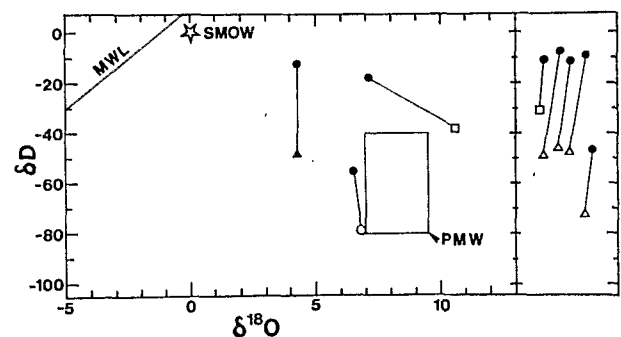


FIG. 46. δD vs. $\delta^{18}\text{O}$ diagram for silicates from the Salau deposit (data from Toulhoat, 1982, and Guy et al., 1988). Open circle = amphibole, open triangles = biotite, black triangle = chlorite, open squares = muscovite, black circles = calculated water, MWL = meteoric water line, PMW = primary magmatic water (from Guy et al., 1988). At the right are shown the δD for some silicates for which $\delta^{18}\text{O}$ has not been determined.

fluid, which appears to have been at or near equilibrium with the carbonate host rock and mainly available in the system during the main hydrothermal stage and ore deposition, whereas the first one would correspond to the saline aqueous fluid, which appears to have been at or near equilibrium with the intrusive rocks and was available in the system during all the stages of formation of the Salau deposit.

S isotope compositions of sulfides

The $\delta^{34}\text{S}$ values for pyrrhotite, chalcopyrite, and sphalerite from the Salau deposit are given in Figure 47 (Guy, 1979, 1980). The ranges of $\delta^{34}\text{S}$ values are low for each mineral: 0.4 to 1.9 per mil for the pyrrhotite, 0.7 to 1.4 per mil for the chalcopyrite (one value at 2.4‰). Pyrrhotite and chalcopyrite appear to be isotopically at disequilibrium and the difference in S isotope compositions between both minerals cannot be used as a geothermometer (e.g. Ohmoto and Rye, 1979).

The $\delta^{34}\text{S}$ value of the total sulfur in solution can be estimated from the mineral analysis and knowledge of temperature, pH, f_{O_2} , and composition of the fluid (e.g., Ohmoto, 1986). For the early hydrothermal stage (formation of the pyrrhotite-scheelite-quartz \pm chalcopyrite assemblage), the temperature and the fugacities of O_2 and S_2 have been estimated above. The pH was either neutral or slightly basic in the carbonate host rocks because of the stability of pyrrhotite and calcite. In such conditions H_2S is the almost exclusive S species in the fluid and the $\delta^{34}\text{S}$ value of sulfur in solution may be estimated at 2 ± 1 per mil for $T = 350^\circ$ to 400°C . Such a $\delta^{34}\text{S}$ value of the fluid

is generally interpreted to be of magmatic or deep-seated origin (Taylor and O'Neil, 1977; Ohmoto and Rye, 1979; Guy, 1979, 1980; Ohmoto, 1986).

A single value is available for the $\delta^{34}\text{S}$ of the sedimentary host rock (pyritic shales of the Mont Rouch Series; Guy, 1979, 1980). The obtained value (-11‰) seems not to be consistent with a local sedimentary origin for sulfur. However, the existence of two contemporaneous fluids suggests that the calculated $\delta^{34}\text{S}$ value of the fluid may represent the result of a mixture between sulfur derived from a magmatic or deep-seated region and sulfur of sedimentary origin. As suggested by Guy (1979, 1980), the fact that the $\delta^{34}\text{S}$ values obtained in Salau are lower than those obtained for the Costabonne and Lacourt skarn-type scheelite deposits would be consistent with this hypothesis.

Summary: The Evolution of the Ore

The skarns and ores at Salau were formed in two stages.

The first one corresponds to the development of hedenbergite skarns in pure, graphite-bearing limestone. Similar skarns formed on calc-silicate hornfels, but in this case, a magnesium-rich zone appeared between the hedenbergite zone and the unmetamorphosed hornfels. The garnet of this early skarn stage is nearly pure grossular. In the intergranular spaces, and in equilibrium with the hedenbergite, a quartz-calcite-pyrrhotite-scheelite paragenesis precipitated at a somewhat later substage. The WO_3 content was at most 0.4 percent. The temperatures of this first stage were in the range 540° to 450°C . The fluids were of very high salinity and may be of magmatic origin.

The second stage corresponds to alteration of the early-stage skarns and of the granite. No new development of skarns in limestones is observed at this stage. It may be divided in three substages: (1) epidotization of grossularite garnet and feldspars of endoskarns, (2) development of a red garnet of mixed grossularite-almandine-spessartite composition, in veins and along the margin of the first-stage skarns, where it was in contact with limestone, and (3) a main stage of development of scheelite, sulfides (mostly pyrrhotite and arsenopyrite), hydrous silicates (epidote, amphibole, chlorite), quartz, and calcite. The WO_3 content of the ore is commonly higher than 1 percent. The gold content may reach locally 10 g/metric ton.

The fluids responsible of this second stage appear to have been in equilibrium with the carbonate host rocks and in disequilibrium with the silicate rocks. The range of temperatures found for this second stage varies from 450° to 350°C . The increase in scheelite content at the contact with the limestone (marble line) is thought to be due to the mixing of the two previous types of fluids as suggested by the existence of type

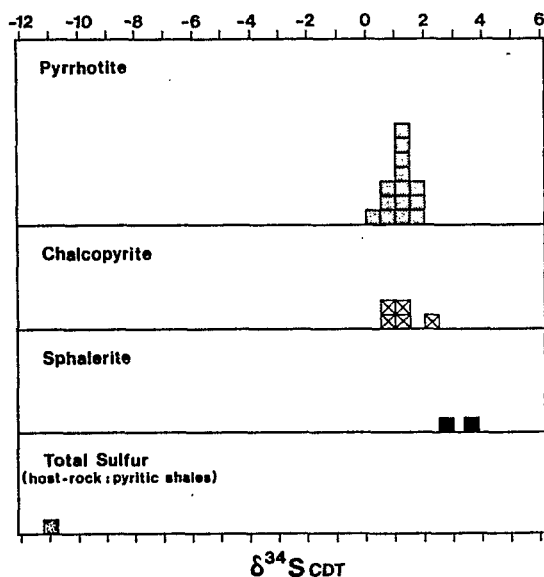


FIG. 47. $\delta^{34}\text{S}_{\text{CDT}}$ of sulfides from the Salau deposit (data from Guy, 1979, 1980).

III fluid inclusions. Local evolution in closed systems at a later stage is responsible for the development of pyrite, and locally, andradite.

Acknowledgments

We thank the Société Minière d'Anglade, J. Faure, manager of the mine, and L. Nansot, chief geologist, for their support during our numerous stays in the mine. In particular, L. Nansot kindly provided many unpublished mining maps, sections, and data on the drilling, ore grades, and reserves. The successive research programs dealing with the Salau deposit have been supported by grants from the Direction Générale de la Recherche Scientifique et Technique (DGRST-France), the Centre National de la Recherche Scientifique (CNRS-France), and the European Economic Community. The authors are especially indebted to *Economic Geology* referees for their very careful reviews of the manuscript.

REFERENCES

- Arnold, R. G., 1966, Mixtures of hexagonal and monoclinic pyrrhotites and the measurement of the metal content of pyrrhotite by X-ray diffraction: *Am. Mineralogist*, v. 51, p. 1221-1227.
- Autran, A., and Guitard, G., 1969, Mise en évidence de nappes hercyniennes de style pennique dans la série métamorphique du massif du Roc de France (Pyrénées Orientales): Liaison avec la nappe du Canigou: *Acad. Sci. [Paris] Comptes Rendus*, v. 269, p. 2497-2499.
- Autran, A., Guitard, G., and Fonteilles, M., 1970, Relations entre les intrusions de granitoïdes, l'anatexis et le métamorphisme régional, considérés principalement du point de vue du rôle de l'eau: cas de la chaîne hercynienne des Pyrénées Orientales *Geol. Soc. France, Bull. Ser. 7*, v. 12, p. 673-731.
- Autran, A., Derré, C., Fonteilles, M., Guy, B., Soler, P., and Toulhoat, P., 1980, Génèse des skarns à tungstène dans les Pyrénées: *Bur. Recherches Geol. Min. Mem.*, no. 99, p. 193-319.
- Barton, P. B., Jr., and Skinner, B. J., 1979, Sulfide mineral stabilities, In Barnes, H. L., ed., *Geochemistry of hydrothermal ore deposits*, 2nd ed.: New York, John Wiley Sons, p. 278-403.
- Ben Othman, D., Polvé, M., and Allègre, C. J., 1984, Nd-Sr isotopic compositions of granulites and constraints of the evolution of the lower crust: *Nature*, v. 307, p. 510-515.
- Bodin, J., and Ledru, P., 1986, Nappes hercyniennes précoces à matériel dévonien hétéropique dans les Pyrénées Ariégeoises.: *Acad. Sci. [Paris] Comptes Rendus*, v. 302, ser. 2, no. 15, p. 969-974.
- Boissonnas, J., and Autran, A., 1974, Succession des déformations de la région du Pic de Maubermé (Pyrénées centrales) au cours de l'orogénèse hercynienne: *Bur. Recherches Geol. Min. Bull.*, sec. II, no. 1, and 1/50 000 geologic map "Pic de Maubermé," v. 19, p. 48.
- Bowman, J. R., Covert, J. J., Clark, A. H., and Mathieson, G. A., 1985a, The CanTung E Zone scheelite skarn orebody, Tungsten, Northwest Territories: Oxygen, hydrogen, and carbon isotope studies: *ECON. GEOL.* v. 80, p. 1872-1895.
- Bowman, J. R., O'Neil, J. R., and Essene, E. J., 1985b, Contact skarn formation at Elkhorn, Montana. II: Origin and evolution of C-O-H skarn fluids: *Am. Jour. Sci.*, v. 285, p. 621-660.
- Brown, P. E., Bowman, J. R., and Kelly, W. C., 1985, Petrologic and stable isotope constraints on the source and evolution of skarn-forming fluids at Pine Creek, California: *ECON. GEOL.*, v. 80, p. 72-95.
- Burt, D. M., 1972, Mineralogy and geochemistry of Ca-Fe-Si skarn deposits: Unpub. Ph.D. thesis, Harvard Univ., 256 p.
- Burton, J. C., Taylor, L. A., and I-Ming, Chou, 1982, The f_{O_2} -T and f_{S_2} -T stability relations of hedenbergite and of hedenbergite-johannsenite solid solutions: *ECON. GEOL.*, v. 77, p. 764-783.
- Caralp, L., 1888, Etudes géologiques sur les Hauts Massifs des Pyrénées Centrales (Haute Ariège, Haute Garonne, Vallée d'Aran): Unpub. Ph.D. thesis, Univ. Toulouse, 512 p.
- Cavet, P., 1957, Le Paléozoïque de la zone axiale des Pyrénées orientales françaises: *Service Carte Géol. France Bull.*, ser. 4, v. 354, 216 p.
- Charuau, D., 1974, Relations entre les minéralisations plombo-zincifères et la tectonique superposée du district de Hoque-Rabé, Saubé, Carboire (Pyrénées Ariégeoises): Unpub. Ph.D. thesis, Univ. Paris 6, 134 p.
- Cygan, C., Perret, M. F., and Raymond, D., 1981, Le Dévonien et le Carbonifère du "synclinal de Villefranche de Conflent" (Pyrénées orientales, France). Datation par conodontes et conséquences structurales: *Bur. Recherches Geol. Min. Bull.*, ser. 2, v. 2, p. 113-118.
- Cocheric, A., 1985, Interaction manteau-croûte: son rôle dans la genèse d'associations calco-alcalines, contraintes géochimiques (éléments en traces et isotopes du strontium et de l'oxygène): *Bur. Recherches Geol. Min.: Doc.* 90, 246 p.
- Deines, P., 1980, The carbon isotopic composition of diamonds: Relationship to diamond shape, color, occurrence and vapor composition: *Geochim. et Cosmochim. Acta*, v. 44, p. 943-962.
- Deramond, J., 1970, Tectoniques superposées dans le Paléozoïque du Haut Salat (Pyrénées Ariégeoises): Unpub. Ph.D. thesis, Univ. Toulouse, 227 p.
- Derré, C., 1973, Relations chronologiques entre la mise en place du granite de Salau (Haute vallée du Salat, Pyrénées Ariégeoises) et les déformations du Paléozoïques de la région: *Acad. Sci. [Paris] Comptes Rendus*, v. 277, sér. D, p. 1279-1281.
- 1978, Le gisement de scheelite de Salau dans son cadre géologique (Pyrénées): *Sci. Terre, Nancy*, v. 22, no. 1, p. 5-68.
- 1982, La province à Sn-W ouest-européenne. Histoire de divers types de gisements du Massif Central, des Pyrénées et du Portugal. Distribution des gisements: Unpub. Ph.D. thesis, Univ. Paris 6, 766 p.
- Derré, C., and Krylatov, S., 1976, Comparaison entre la série de Salau (Ariège) et d'autres séries du Dévonien de la partie centrale des Pyrénées. Un caractère original de la partie inférieure du Dévonien: Présence de phosphates: *Acad. Sci. [Paris] Comptes Rendus*, v. 282, ser. D, p. 2051-5054.
- Derré, C., Lafitte, M., and Maury, R., 1984, Etude des minéralisations sulfurées du gisement de Salau, Pyrénées (France) et de ses environs: *Mineralium Deposita*, v. 19, p. 176-182.
- Dommanget, A., 1977, Le cadre géologique des niveaux minéralisés (Pb-Zn) du Paléozoïque de la zone axiale des hautes Pyrénées Ariégeoises (secteur d'Aulus-Port d'Aula): Unpub. Ph.D. thesis, Univ. Paris 6, 205 p.
- Einaudi, M. T., Meinert, L. D., and Newberry, R. J., 1981, Skarn deposits: *ECON. GEOL. 75TH ANNIV. VOL.*, p. 317-391.
- Ernst, W. G., 1966, Synthesis and stability relations of ferrotremolite: *Am. Jour. Sci.*, v. 264, p. 37-65.
- Fonteilles, M., 1976, Essai d'interprétation des compositions chimiques des roches d'origine métamorphique et magmatique du massif hercynien de l'Agly (Pyrénées Orientales): Unpub. Ph.D. thesis, Univ. Paris 6, 685 p.
- 1979, Les mécanismes de la métasomatose: *Bull. Minéralogie*, v. 101, p. 166-194.
- 1962, Contribution à l'étude des skarns de Kamioka, préfecture de Gifu, Japon: *Tokyo Univ. Fac. Sci. Jour.*, v. 14, p. 153-227.

- Fonteilles, M., and Garcia, D., 1985, Le grenat mixte grossulaire—almandin (spessartine) comme indicateur d'une source magmatique proche dans les gîtes de type skarns à tungstène. *Acad. Sci. [Paris] Comptes Rendus*, v. 300, p. 807–810.
- Fonteilles, M., and Guitard, G., 1977, Influence des noyaux de socle précambrien sur le métamorphisme et la structure profonde de l'orogène hercynien des Pyrénées. Comparaison avec des régions voisines, in "La chaîne varisque d'Europe moyenne et occidentale": Rennes, France, Coll. interne CNRS no. 243, p. 81–87.
- Fonteilles, M., and Machairas, G., 1968, Eléments d'une description pétrographique et métallogénique du gisement de scheelite de Salau (Ariège): *Bur. Recherches Geol. Min. Bull.*, sér. 2, no. 3, p. 62–85.
- Fonteilles, M., Guy, B., and Soler, P., 1980, Etude du processus de formation des gîtes de skarns de Salau et Costabonne: *Bur. Recherches Geol. Min. Mem.*, no. 99, p. 259–282.
- Fonteilles, M., Nansot, L., Soler, P., and Zahm, A., 1988, Ore controls for the Salau Scheelite deposit (Ariège-France): Evolution of the ideas and present stage of knowledge: *Soc. Geology Appl. Mineral Deposits Spec. Pub.* 6, Berlin-New York: Springer-Verlag, p. 95–116.
- Friedman, I., and O'Neil, J. R., 1977, Compilation of stable isotope fractionation factors of geochemical interest: *U.S. Geol. Survey Prof. Paper* 440-KK, 12 p.
- Froese, E., and Gunter, A. E., 1976, A note on the pyrrhotite-sulfur vapor equilibrium: *ECON. GEOL.*, v. 71, p. 1589–1594.
- Gamble, R. P., 1982, An experimental study of sulfidation reactions involving andradite and hedenbergite: *ECON. GEOL.*, v. 77, p. 784–797.
- Gordon, T. M., and Greenwood, H. J., 1971, The stability of grossularite in H₂O-CO₂ mixtures: *Am. Mineralogist*, v. 56, p. 1674–1688.
- Graham, C. M., Harmon, R. S., and Sheppard, S. M. F., 1984, Experimental hydrogen isotope studies—I. Systematics of hydrogen isotope exchange between amphibole and water: *Am. Mineralogist*, v. 69, p. 128–138.
- Graham, C. M., Viglino, J. A., and Harmon, R. S., 1987, Experimental study of hydrogen-isotope exchange between aluminous chlorite and water and of hydrogen diffusion in chlorite: *Am. Mineralogist*, v. 72, p. 566–579.
- Guitard, G., 1964, Un exemple de structure en nappe de style pennique dans la chaîne hercynienne: Les gneiss stratoides du Canigou (Pyrénées Orientales): *Acad. Sci. [Paris] Comptes Rendus*, v. 258, p. 4597–4599.
- 1970, Le métamorphisme hercynien mésozoal et les gneiss ocellés du Massif du Canigou (Pyrénées Orientales): *Bur. Recherches Geol. Min. Mem.*, no. 63, 317 p.
- Gustafson, W. I., 1974, The stability of andradite, hedenbergite, and related minerals in the system Ca-Fe-Si-O-H: *Jour. Petrology*, v. 15, p. 455–496.
- Guy, B., 1979, Pétrologie et géochimie isotopique (S, C, O) des skarns de Costabonne: Unpub. Ph.D. thesis, Ecole Mines Paris, 240 p.
- 1980, Géochimie isotopique du soufre, du carbone et de l'oxygène des skarns des Pyrénées: *Bur. Recherches Geol. Min. Mem.*, no. 99, p. 282–292.
- 1988, Contribution à l'étude des skarns de Costabonne (Pyrénées Orientales, France) et à la théorie de la zonation métasomatique: Unpub. Ph.D. thesis, Univ. Paris 6, 645 p.
- Guy, B., Sheppard, S. M. F., Fouillac, A. M., Le Guyader, R., Toulhoat, P., and Fonteilles, M., 1988, Geochemical and isotopic (H, C, O, S) studies of barren and tungsten-bearing skarns of the French Pyrenees: *Soc. Geology Appl. Mineral Deposits Spec. Pub.* 6, Berlin-New York, Springer-Verlag, p. 53–75.
- Helgeson, H. C., Delany, J. M., Nesbitt, H. W., and Bird, D. K., 1978, Summary and critique of the thermodynamic properties of minerals: *Am. Jour. Sci.*, v. 278A, 229 p.
- Herskowitz, M., and Kisch, H., 1984, An algorithm for finding composition, molar volume and isochores of CO₂-CH₄ fluid inclusions from T_h and T_m (for T_h < T_m): *Geochim. et Cosmochim. Acta*, v. 48, p. 1581–1587.
- Hochella, M. F., Jr., Liou, J. G., Keskinen, M. J., and Kim, H. S., 1982, Synthesis and stability relations of magnesium idocrase: *ECON. GEOL.*, v. 77, p. 798–808.
- Holdaway, M. J., 1972, Thermal stability of Al-Fe epidote as a function of fO₂ and Fe content: *Contr. Mineralogy Petrology*, v. 37, p. 307–340.
- Holland, H. D., 1965, Some applications of thermodynamical data to problems of ore deposits II. Mineral assemblages and the composition of the ore-forming fluids: *ECON. GEOL.*, v. 60, p. 1101–1166.
- Hunt, I. A., and Kerrick, D. M., 1977, The stability of sphene; experimental redetermination and geologic implications: *Geochim. et Cosmochim. Acta*, v. 41, p. 279–288.
- Iiyama, J. T., 1984, Hydrothermal solution-mineral equilibria as clue for studies of geochemical transport phenomena in the earth's crust, in Sunagawa, I., ed., *Material sciences of the Earth's interior*: Tokyo, Terra Sci. Pub. Co., p. 493–513.
- Iiyama, J. T., and Fonteilles, M., 1981, Mesozoic granitic rocks of Southern Korea reviewed from major constituents and petrography: *Mining Geology*, v. 31, p. 281–295.
- Ito, J., and Arem, E., 1970, Idocrase: Synthesis, phase relations and crystal chemistry: *Am. Mineralogist*, v. 55, p. 880–912.
- Jacobs, G. K., and Kerrick, D. M., 1981, Methane: An equation of state with application to the ternary system H₂O-CO₂-CH₄: *Geochim. et Cosmochim. Acta*, v. 45, p. 607–614.
- Johan, Z., Campiglio, C., Lagache, M., LeBel, L., and McMillan, W. J., 1980, Porphyres cuprifères dans leur contexte magmatique: *Bur. Recherches Geol. Min. Mem.*, no. 99, p. 9–190.
- Kaelin, J.-L., 1979, Le grenat tardif dans le gisement de scheelite de Salau: *Ecole des Mines de Saint Etienne*, Unpub. rept. 25 p.
- 1982, Analyse structurale du gisement de scheelite de Salau (Ariège-France): Unpub. Ph.D. thesis, Ecole des Mines de Saint Etienne, 217 p.
- Keith, M. L., and Weber, J. N., 1964, Carbon and oxygen isotopic composition of selected limestones and fossils: *Geochim. et Cosmochim. Acta*, v. 28, p. 1787–1816.
- Kerrick, D. M., 1977, The genesis of zoned skarns in the Sierra Nevada, California: *Jour. Petrology*, v. 18, p. 144–181.
- Kerrick, D. M., and Jacobs, G. K., 1981, A modified Redlich-Kuung equation for H₂O, CO₂ and H₂O-CO₂ mixtures at elevated pressures and temperatures: *Am. Jour. Sci.*, v. 281, p. 735–767.
- Kerrick, D. M., Crawford, K. E., and Randazzo, A. F., 1973, Metamorphism of calcareous rocks in three roof-pendants in the Sierra Nevada, California: *Jour. Petrology*, v. 14, p. 303–325.
- Korzinskii, D. S., 1969, Theory of metasomatic zoning (translation Jean Agrell): Oxford, Clarendon Press, 162 p.
- Kretschmar, U., and Scott, S. D., 1976, Phase relations involving arsenopyrite in the system Fe-As-S and their application: *Canadian Mineralogist*, v. 14, p. 364–386.
- Krier-Schellen, A.-D., 1988, Etude microthermométrique des inclusions fluides des différentes paragenèses du gisement de scheelite (tungstène) de Salau (Pyrénées Ariégeoises, France): Unpub. Ph.D. thesis, Univ. Catholique Louvain-la-Neuve (Belgium), 131 p.
- Laumonier, B., and Guitard, G., 1986, Le Paléozoïque inférieur de la moitié orientale des Pyrénées. Essai de synthèse: *Acad. Sci. [Paris] Comptes Rendus*, v. 302, p. 473–478.
- Lecouffe, J., 1987, Les épisodes de fracturation dans le gisement de scheelite de Salau (Ariège). Caractères géométriques et pétrologiques, relation avec la minéralisation et implications minérales: Unpub. Ph.D. thesis, Univ. Paris 6, 152 p.

- Leterrier, J., 1972, Etude pétrographique et géochimique du Massif granitique du Quérigut (Ariège): *Sci. Terre, Nancy, Mem.* 23, 292 p.
- Liou, J. G., 1971, Synthesis and stability relations of prehnite $\text{Ca}_2\text{Al}_2\text{Si}_2\text{O}_{10}(\text{OH})_2$: *Am. Mineralogist*, v. 56, p. 507-531.
- 1973, Synthesis and stability relations of epidote $\text{Ca}_2\text{Al}_2\text{FeSi}_3\text{O}_{12}(\text{OH})$: *Jour. Petrology*, v. 14, p. 381-413.
- 1974, Stability relations of andradite-quartz in the system Ca-Fe-Si-O-H: *Am. Mineralogist*, v. 59, p. 1016-1025.
- Liou, J. G., Kim, H. S., and Maruyama, S., 1983, Prehnite—epidote equilibria and their petrologic applications: *Jour. Petrology*, v. 24, p. 321-342.
- Losantos, M., Palau, J., and Sanz, J., 1985, Considerations about Hercynian thrusting in the Marimanya Massif (Central Pyrenees): *Terra Cognita*, v. 6, p. 22.
- Moore, J. G., 1959, The quartz diorite boundary line in the western United States: *Jour. Geology*, v. 67, p. 198-210.
- Moret, J.-F., and Weyant, M., 1986, Datation de l'Émsien-Dévonien moyen des calcaires de Campaüs et des schistes d'Escala Alta, équivalents occidentaux de la "série de Salau" (zone axiale pyrénéenne, Haute Noguera-Pallaresa, province de Lerida, Espagne). Conséquences structurales: *Acad. Sci. [Paris] Comptes Rendus*, v. 302, p. 353-356.
- Newberry, R. J., 1983, The formation of subcalcic garnet in scheelite-bearing skarns: *Canadian Mineralogist*, v. 21, p. 529-544.
- Newton, R. C., 1966, Some calc-silicate equilibrium relations: *Am. Jour. Sci.*, v. 264, p. 204-222.
- Ohmoto, H., 1986, Stable isotope geochemistry of ore deposits: *Rev. Mineralogy*, v. 16, p. 491-559.
- Ohmoto, H., and Rye, R. O., 1979, Isotopes of sulfur and carbon, in Barnes, H. L., ed., *Geochemistry of hydrothermal ore deposits*, 2nd ed.: New York, Wiley Intersci., p. 509-567.
- Palau, J., Losantos, M., and Sanz, J., 1989, Geologia del Massif de Marimanya: *Catalunya Geol. Servei*.
- Perchuk, L. L., and Arenovich, L. Ya., 1979, Thermodynamics of mineral of variable compositions: Andradite-grossularite and pistacite-clinozoisite solid solutions: *Physics Chemistry Minerals*, v. 5, p. 1-14.
- Pettijohn, P. F., Potter, P. E., and Siever, R., 1972, Sands and sandstones: Berlin, Springer-Verlag, 618 p.
- Potter, R. W., and Brown, D. L., 1977, The volumetric properties of aqueous sodium chloride solutions from 0° to 500°C at pressures up to 2000 bars based on a regression of available data in the literature: *U.S. Geol. Survey Bull.* 1421-C, 36 p.
- Raimbault, L., 1981, Pétrographie et géochimie des roches du massif granodioritique de Salau (Pyrénées): *Ecole des Mines de Saint Etienne, France, unpub. report*, 85 p.
- Raimbault, L., and Kaelin, J.-L., 1987, Géologie, pétrographie et géochimie de la granodiorite de la Fourque et de ses faciès hydrothermalisés associés aux skarns à scheelite de Salau (Pyrénées, France): *Bull. Minéralogie*, 110, 6, p. 633-644.
- Rau, H., 1976, Energetics of defects formations and interaction in pyrrhotite Fe_{1-x}S and its homogeneity range: *Jour. Physics Chem. Solids*, v. 37, p. 425-429.
- Raymond, D., 1980, Découverte d'une unité allochtone varisque dans le haut pays de Sault (zone axiale pyrénéenne, confins de l'Aude et de l'Ariège): *Sommaire Soc. Géol. France, Compte Rendus ser. 7*, v. 22, p. 250-252.
- Robie, R. A., and Waldbaum, D. R., 1968, Thermodynamic properties of mineral and related substances at 298.15 K (25.0°C) and one atmosphere (1.013 bars) pressure and at higher temperatures: *U.S. Geol. Survey Bull.* 1259, 256 p.
- Robie, R. A., Hemingway, B. S., and Fisher, J. R., 1978, Thermodynamic properties of mineral and related substances at 298.15 K and 1 bar (10^5 pascals) pressure and at higher temperatures: *U.S. Geol. Survey Bull.* 1452, 458 p.
- Robinson, G. R., Haas, J. L., Schafer, C. M., and Haselton, H. T., 1983, Thermodynamic and thermophysical properties of selected phases in the $\text{MgO-SiO}_2\text{-H}_2\text{O-CO}_2$, $\text{CaO-Al}_2\text{O}_3\text{-SiO}_2\text{-H}_2\text{O-CO}_2$ and $\text{Fe-FeO-Fe}_2\text{O}_3\text{-SiO}_2$ chemical systems, with special emphasis on the properties of basalts and their mineral components: *U.S. Geol. Survey Open-File Rept.* 83-0079, 465 p.
- Ryzhenko, B. N., and Malinin, S. D., 1971, The fugacity rule for the systems $\text{CO}_2\text{-H}_2\text{O}$, $\text{CO}_2\text{-CH}_4$, $\text{CO}_2\text{-N}_2$ and $\text{CO}_2\text{-H}_2$: *Geochemistry Internat.*, v. 8, p. 562-574.
- Sharp, Z. D., Essene, E. J., and Kelly, W. C., 1985, A re-examination of the arsenopyrite geothermometer: Pressure considerations and applications to natural assemblages: *Canadian Mineralogist*, v. 23, p. 517-534.
- Sheppard, S. M. F., 1986, Characterization and isotopic variations in natural waters: *Rev. Mineralogy*, v. 16, p. 165-183.
- Sheppard, S. M. F., and Dawson, J. B., 1975, Hydrogen, carbon and oxygen isotope studies of megacrysts and matrix minerals from Lesotho and South African kimberlites, in Ahrens, L. H., Dawson, J. B., Duncan, A. R., and Erlank, A. J., eds., *Physics and chemistry of the earth: New York, Pergamon Press*, vol. 9, p. 747-763.
- Shimazaki, H., 1977, Grossular-spessartine-almandine garnets from some Japanese scheelite skarns: *Canadian Mineralogist*, v. 15, p. 74-80.
- Slaughter, J., Kerrick, D. M., and Wall, V. J., 1975, Experimental and thermodynamic study of equilibria in the system $\text{CaO-MgO-SiO}_2\text{-H}_2\text{O-CO}_2$: *Am. Jour. Sci.*, v. 275, p. 143-162.
- Soler, P., 1977, Pétrographie, thermochimie et métallogénie du gisement de scheelite de Salau (Pyrénées Ariégeoises-France): Unpub. Ph.D. thesis, Ecole des Mines de Paris, 220 p.
- Soler, P., and Fonteilles, M., 1980a, Etude pétrologique du gisement de Salau et de son enveloppe immédiate: *Bur. Recherches Geol. Min. Mem.* no. 99, p. 217-230.
- 1980b, Minéralisation et altération hydrothermale du gisement de Salau: *Bur. Recherches Geol. Min. Mem.* no. 99, p. 231-250.
- Susuoki, T., and Epstein, S., 1976, Hydrogen isotope fractionation between OH-bearing minerals and water: *Geochim. et Cosmochim. Acta*, v. 40, p. 1229-1240.
- Swanenberg, H. E. C., 1979, Phase equilibria in carbonic systems and their application to freezing studies of fluid inclusions: *Contr. Mineralogy Petrology*, v. 68, p. 303-306.
- Taylor, H. P., Jr., 1974, The application of oxygen and hydrogen isotope studies to problems of hydrothermal alteration and ore deposition: *ECON. GEOL.*, v. 69, p. 843-883.
- Taylor, B. E., and Liou, J. G., 1978, The low temperature stability of andradite in C-O-H fluids: *Am. Mineralogist*, v. 63, p. 378-393.
- Taylor, B. E., and O'Neil, J. R., 1977, Stable isotope studies of metasomatic Ca-Fe-Al-Si skarns and associated metamorphic and igneous rocks: *Contr. Mineralogy Petrology*, v. 63, p. 1-49.
- Taylor, H. P., Jr., Frechen, J., and Degens, E. T., 1967, Oxygen and carbon isotope studies of carbonatites from the Laacher See District, West Germany and the Alno District, Sweden: *Geochim. et Cosmochim. Acta*, v. 31, p. 407-430.
- Toulhoat, P., 1982, Pétrographie et géochimie des isotopes stables (D/H, $^{18}\text{O}/^{16}\text{O}$, $^{13}\text{C}/^{12}\text{C}$, $^{34}\text{S}/^{32}\text{S}$) des skarns du Quérigut—comparaison avec les skarns à scheelite des Pyrénées: Unpub. Ph.D. thesis, Univ. Paris 6, 268 p.
- Toulmin, P. III, and Barton, P. B., Jr., 1964, A thermodynamic study of pyrite and pyrrhotite: *Geochim. et Cosmochim. Acta*, v. 28, p. 641-671.
- Uchida, E., and Iiyama, J. T., 1980, Echanges ioniques Fe-Mg entre la série diopside—hedenbergite et une solution hydrothermal [abs.]: *Internat. Geol. Cong. 26th, Paris, 1980*, v. 1, Résumés, p. 97.

- Valley, J. W., 1986, Stable isotope geochemistry of metamorphic rocks: *Rev. Mineralogy*, v. 16, p. 445-489.
- Van Marcke de Lummen, G., 1983, *Pétrologie et géochimie des skarnoïdes du site tungstifère de Costabonne (Pyrénées Orientales)*: Unpub. Ph.D. thesis, Univ. Catholique Louvain-la-Neuve (Belgium), 293 p.
- Vitrac-Michard, A., and Allègre, C. J., 1975, A study of the formation and history of a piece of continental crust by ^{87}Rb - ^{87}Sr method: The case of the French Oriental Pyrenees: *Contr. Mineralogy Petrology*, v. 50, p. 257-285.
- Walther, J. V., and Helgeson, H. C., 1980, Description and interpretation of metasomatic phase relations at high pressures and temperatures: 1. Equilibrium activities of ions species in nonideal mixtures of CO_2 and H_2O : *Am. Jour. Sci.*, v. 280, p. 575-606.
- Yund, R. A., and Hall, H. T., 1969, Hexagonal and monoclinic pyrrhotites: *ECON. GEOL.*, v. 64, p. 420-423.
- Zahn, A., 1987a, *Pétrologie, minéralogie et géochimie des cornéennes calciques et des skarns minéralisés dans le gisement de scheelite de Salau (Ariège, France)*: Unpub. Ph.D. thesis, Univ. Paris 6, 330 p.
- 1987b, The compositional evolution of calc silicates from the Salau skarn deposit (Ariège, Pyrénées): *Bull. Minéralogie*, v. 110, p. 623-632.
- Zandvliet, J., 1960, The geology of the Upper salat and Pallaresa Valleys, central Pyrenees, France/Spain: *Leidse Geol. Meded. decl.* v. 25, p. 1-128.